STATEMENT

Name : Mazin Ali Fargalla Gumma

ELTE Faculty of Science, Field of studies : Materials Science

Title of the thesis : Investigation of BSA/gold bioconjugate / poly(N-isoprylacrylamide) microgel interaction.

I hereby declare as the author of this thesis, that it is a product of my own and that it contains my own ideas. I used the standard rules for references and quotations consistently. I never used other people's idea without proper reference.

Budapest, 4th January 2021

Mazin Ali

Signature

Investigation of BSA/gold bioconjugate / poly(N-isoprylacrylamide) microgel interaction

M.Sc. Dissertation Work

Mazin Ali Fargalla Gumma

Supervisor: Dr. Varga Imre

Department of Physical Chemistry
Institute of Chemistry
Eötvös Loránd University

2020

Contents **Pages No**

Acknowledgments

First and foremost, I would like to thank the ‘Almighty’ who has given me patience, courage and all the things from time to time to complete this thesis, I express my heartfelt gratitude and sincere thanks to my research guide Prof. *Varga Imre* for all his guidance, support and patience. His sincere interests in science have been a great inspiration to me. I am greatly impressed by his passion, hard work, speed and discipline in research. It has been a great pleasure for being one of his students. Also, I would like to thank *Anna Harsanyi* I extend my gratitude to *the family of the colloidal chemistry laboratory* who have provided technical support and assistance during this project. Although only my name will appear on the cover page of this thesis, many people have contributed in its production. I owe my gratitude to all those who have stood by me during tough times and have made this thesis possible.

Last but not the least I would like to thank my family members who stood by me and have always extended their help and love whenever I needed them the most.

MAZIN ALI

Abstract

Microgels are unique three-dimensional polymeric network, they can swell or collapse in a solvent such as water under certain external stimuli such as temperature, light, enzymes, pH, magnetic and electric fields, etc. Microgels have considered as a smart material since their properties such as the volume, shape and their interactions are tunable by different stimuli as well as they are biocompatible soft materials. They have drawn much attention due to the vast range of novel disciplines such as biosensors. One of the most used responsive microgels is PNIPAAm which has non-linear reversible response at 32 C. PNIAAm copolymerized with Allylamine, the obtained copolymer exhibit fully VPT at 32.84 C. the hydrodynamic size was measured by using dynamic light scattering, while the electrophoretic mobility of PNIPAAm-co-Ala particles was measured by using Zetasizer instrument, the spectrums of the supernatant solutions were measured by using UV-Vis spectrophotometer. PNIPAAm-co-Ala is promising microgel that can be used as a biological candidate to incorporate with Boven serum albumin/gold ions bioconjugate system. The Au(III) are reduced and stabilized by BSA, BSA/Au bioconjugate has a red fluorescence emission depends on the BSA structural conformation which is depends on the pH of the medium. Herein, to obtain a stable fluorescence biosensor probe the binding between PNIPAAm-co-Ala and BSA in different pH have been tested as well as the entrapping of Au(III) into PNIPAAm-co-Ala, finally to investigate the red fluorescence of PNIPAAm-co-Ala/BSA/Au bioconjugate system two series of different pH samples were prepared and placed into bath at 37 C for 2 hours then aged at room temperature for two days, then the samples were centrifuged to obtain the supernatant solution and the red fluorescence was investigated.

Abbreviation

pKa, pKb	Logarithm of acid, base dissociation constant
PNIPAAm	Poly (N-Isopropylacrylamide)
Ala	Allylamine
BSA	Bovine Serum Albumin
Au NPs/ NCs	Gold nanoparticles/nanocluster
LCST	Low critical solution temperature
UCST	Upper critical solution temperature
VPTT	Volume transition temperature
UV/Vis	Ultraviolet/Visible
TEM	Transmission electron microscopy
SAXS	Small angle x-ray scattering
SANS	Small angle neutron scattering
BIS	N,N-methylene bisacrylamide
SDS	Sodium dodecyl sulfate
V50	2,2’-azobis(2-methylpropionamidine) dihydrochloride

Chapter one

1. Overview

1.1 Materials Science in Medicine and Biological Field

The last thirty years have witnessed real progress in scientific fields especially in chemistry, physics and engineering which have been reflected on materials science field, where the subjects that once had a little connection with each other, have linked. Several remarkable ideas have been resulted in great innovations on the borderline of the various fields. Several pressing issues in science that the scientists currently face are due to either the material's limited availability or the way of these materials are used. Therefore, breakthroughs in materials science extremely affect the technology future.

One of the most interesting things about materials science is that the material properties depend strongly on the particles size, viz the material properties can change dramatically with a small change in particle size. Materials science is a broad interdisciplinary field that spans many of scientific research with the importance of studying the material’s properties changes to understand the behavior of the materials at different environments, that leads to control and gain the desired behavior of bulk materials either through manipulating their structure at molecular level or through influencing in the surrounding environments, which is the main key to designing and discovery of new materials with different properties and different performances. This versatility can be seen in many applications such as biomedical materials, biomedicine, engineering applications physical metallurgy, ceramics, fibers, nanostructured materials, nanocomposites and polymers science. Materials science now offers an opportunity to link the research in advanced materials with the health care and treatment applications. Therefore, through materials science logic it's possible to achieve the desired material

structure, and through well-controlling behavior it can be used in the nanomedicine field thus allowing the innovation and discovery of new various systems, in this regard, biomaterial and nanomedicine science have offered a new way to treat and diagnose biological and medical issues, that includes tissues engineering, drug tracking and delivery systems, regenerative medicine strategies, therapy and diagnosis of a variety of diseases [1,2].

One of the promising materials that have been used widely in most fields especially in biological and nanomedicine applications are polymers.

Polymers are large chain-like molecule of repeating of many small units called monomers. These monomers are joined by strong covalent bonds. Polymers can be found either naturally or they can be synthesized. In this regard, most of the synthesized polymers used today are derived from petroleum, and only a few of these polymers are biocompatible. However, water swollen polymer networks (hydrogels) were found to show high level of biocompatibility with promising functions which make them an ideal candidate in the field of biological applications [3].

1.2 Hydrogels

Gels are coherent semi-solid systems, which contain molecules dispersed in a relatively large amount of a liquid that form a 3D network to ‘solidify’ the system. Based on the liquid used, the gel might be called a lipogel or organogel when the liquid is oil, and hydrogel is conventionally used when the liquid is water .

A hydrogel is an elastic material composed of a 3D network of hydrophilic cross-linked polymeric chains that make hydrogels insoluble in water but makes them absorb water in a large extent. Gels can exhibit a blended property of both solid and liquid phases. The hydrogel water absorption arises from the hydrophilicity of

the network, the existence of hydrophilic functional groups such as, $-NH_2$, $-COOH$, $-OH$, $-CONH_2$, $-CONH$, and $-SO_3H$, on the polymer backbone increase the swelling, while the resistance of dissolution in water comes from the cross-links of network chains.

In recent years, researchers have been developing smart polymer materials, that can change their properties, e.g. their volume in a large extent, in a non-linear, reversible manner in response to an environmental stimulus (temperature, pH, UV-light intensity, and electric field changes. etc.) [4].

The swelling of hydrogel depends on the degree of cross-linked, the chemical composition, the interaction between the water molecules and the polymer network, volume fraction, the concentration of polymer molecular weight, the surfactants used and the effect of salts as well. Thus, some polymers show significant changes in their solubility with varying temperature. When a polymer is soluble in water at low temperature but becomes insoluble at higher temperature, this polymer possesses a characteristic Lower Critical Solution Temperature (LCST). When such a polymer is used to prepare a gel, the polymer network is highly swollen in water at low temperature. However, when the temperature is increased above the LCST, the gel loses its water content and collapses. The gel collapse is a reversible process, when the system is cooled the gel network swells again.

1.3 Properties of Hydrogel

Recently hydrogels have attracted growing attention due to their unique properties. These properties play an important role in determining their application. The properties of hydrogels are classified as physical, mechanical and chemical, and they depend strongly on the conditions of the swelling environment. The most

common properties are the water uptake with high capacity, the swelling behavior, permeability, surface properties, and optical properties.

In 1960 Wichterle and Lim[5] had succeeded to prepare cross-linked HEMA hydrogels, which were potentially biocompatible, and due to their hydrophilic character, they have been of great importance to the biomaterial researchers. Later, Wichterle and Lim succeeded to demonstrate an application of calcium alginate cell encapsulation. In 1980s, Yannas et al, succeeded to make an artificial burn dressings system by incorporating a natural polymer with cartilage into the hydrogel. Hydrogels have an essential role in numerous applications especially in pharmaceutical and medical fields such as artificial skin [6], wound dressings [7], drug and protein delivery system [8], cosmetics [9], personal hygiene product [10] and as besides those, hydrogels can be used in advance industrial application as oil recovery [11], in the biological field such as water treatment [12], biosensors [13], tissue engineering [14] and contact lens [15], in agriculture [16] as well. In the scheme below a simple idea of the water content among polymers chains.

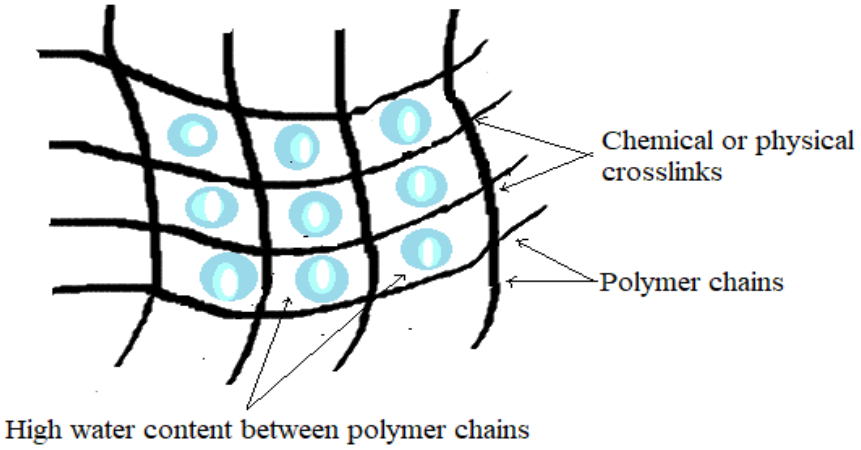

Figure 1.1. shows the chemical or physical crosslinks in hydrogel and the water content [17].

1.4 Technology for Hydrogel Preparation

Hydrogels are water-swollen crosslinked polymeric chains generally prepared from hydrophilic monomers by adopted various technologies to perform the crosslinking copolymerization, such as bulk polymerization, solution polymerization [18], radiation polymerization [19], suspension polymerization [20] and the commonly used technique is free-radical polymerization [21].

1.4.1 Bulk Polymerization

Bulk polymerization have been considered as the simplest polymerization approach in terms of polymer formulation for production of hydrogels. One or more types of monomer is mixed in liquid state, then addition of a radical initiator (ultraviolet or chemical catalyst) which is chosen based on the monomer type, and chain crosslinker if needed is added to the system, This polymerization is carried out in the absence of solvent or dispersant, thus, resulting in high rate and degree of polymerization. The synthesized crosslinked polymer network is always high purity and gives rise to a hard gel with high molecular weight [22]. Acrylic hydrogels of high purity are prepared by this method.

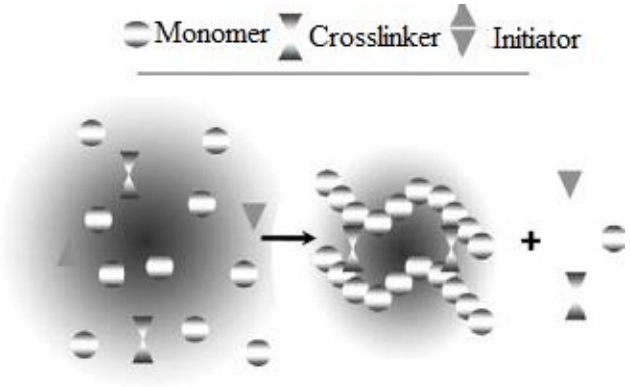

Figure 1.2. scheme illustrate the preparation of hydrogel through bulk polymerization

1.4.2 Solution Polymerization

In the solution polymerization a mixture of monomers and a crosslinker are dissolved into a suitable solvent. To initiate the polymerization UV light or a redox initiator is required. The presence of the solvent is to enhance the heat transfer which is the main difference from bulk polymerization. The solvents used in the polymerization are typically water-ethanol mixture, water, ethanol, and benzyl alcohol. The synthesized gel must be washed to eliminate the impurities, such as soluble monomers, oligomers or the crosslinking agent

1.4.3 Suspension Polymerization

Through this method the synthesized hydrogel is obtained as a powder or microsphere (bead), therefore grifting is not required. The monomer solution is dispersed into non-solvent, to form droplets of monomers and then stabilized. The size of the gel particles can be controlled by adjusting the hydrophilic-hydrophobic balance of each suspension agent. Poly(hydroxyethyl-methacrylate) has been synthesized through this technique [23].

1.4.4 Graft Polymerization

In graft polymerization the monomers are attached covalently to the backbone polymer chain. Therefore, graft polymerization imparts a variety of functional groups to the polymer backbone. Graft polymerization can take place as copolymerization if the attached monomers are differing in type. On the other hand, graft homopolymerization involves only one type of attached monomer. Graft polymerization has been used widely specially to introduce specific properties to the hydrogels. E.g. in the case of hydrogels with relatively weak structure, it is important to enhance the mechanical properties by grafting a polymerizable monomers onto polymer backbone which have functional groups

that can react with the polymerizable monomers. E.g. polyacrylic acid gel exhibit sharp swelling properties but with poor mechanical strength. Thus polyacrylic acid can be grafted onto starch in order to enhance its mechanical properties [24].

1.4.5 Irradiation Polymerization

Crosslinked hydrogels can also be prepared from by using ionizing high energy radiation such as gamma ray to initiate crosslinking. The polymerization is started by radiating the aqueous polymer solution which leads to the formation of radicals and hydroxyl radicals on the polymer chains. The macroradicals on the polymer chain form covalent bonds with each other, which leads to a crosslinked polymer network. The hydrogel synthesized by this method is relatively pure [25].

1.5 Classification of Hydrogels

Hydrogels are classified according to their properties, the preparation methods, type of stimuli that they may be responsive to. Hydrogels may have ionic groups bound to the polymer chains. Thus, they might be anionic or cationic. Smart hydrogels that are responsive to the change in environmental factors of the surrounding medium are classified to physical stimuli responsive hydrogels, chemical stimuli responsive hydrogels and biological stimuli responsive hydrogels.

The type of crosslinking agent might be used as classification criteria as well[17].

The table1 shows the hydrogel classification.

	Main feature	Class	Subclass
Hydrogel	Source	Natural	
		Semi-synthesized	
		Synthesized	
	Preparation	Homopolymeric	
		Copolymeric	
		Interpenetrating	
	Cross linking	Physical	
		chemical	
	Response	Physical	Temperature
			Pressure
			Light
		chemical	pH
			Glucose
			Oxidant
		Biological	Enzyme
			Antigen
			Ligand
	Electrical charge	Anionic	
		Catanionic	
		Nonionic	
	Physical properties	Smart material	
		Conventional	

Table1 shows the classification of hydrogel based on different properties [26].

1.6 Stimuli Responsive Hydrogels

Smart hydrogels have the unique behavior that they respond dramatically to small changes of the surrounding environment (pH, temperature, electric and magnetic field, UV light, etc.). This response could be the change the degree of swelling of the gel Thus, stimuli responsive hydrogels are used widely in drug delivery as their load can be released as the consequence of the changing swelling of the gel. Unfortunately, macroscopic hydrogels have a slow response to changes in medium condition. This problem can be overcome by reducing the size of hydrogels to few hundred of nanometers and preparing nano and microgel particles [27].

Several types of stimuli sensitive gels have been developed, the stimuli might be physical stimuli (e.g. (temperature, pressure, electric or magnetic field, UV light, mechanical stress), chemical stimuli such as pH, ion and specific molecular recognition events, which induce molecular interactions between the components of the system, or biological stimuli that is based on enzymes and receptors [28].

1.6.1 Thermo-sensitive Hydrogels

In many of the recently published papers thermo-sensitive hydrogel are used as stimuli responsive polymer especially in drug delivery research and biosensing. Thermo-sensitive hydrogels are capable to swell or shrink when the temperature of the surrounding medium changes. The reason behind this is generally the existence of both hydrophobic and hydrophilic groups in the polymer structure. The phenomenon of thermo-sensitive behavior arises from the balance between these hydrophilic/hydrophobic groups of the monomers. The temperature change induces the change of interactions between hydrophilic/hydrophobic groups present in the polymer chain and the water molecules. Thus, the solubility of the cross-linked chains also changes, which leads to the swelling or deswelling of the crosslinked

polymer network. Therefore, the hydrogel can go through a volume phase transition. This behavior is characterized by a critical solution temperature CST, which is very important factor to describe the thermo-responsive hydrogel[29] as shown below.

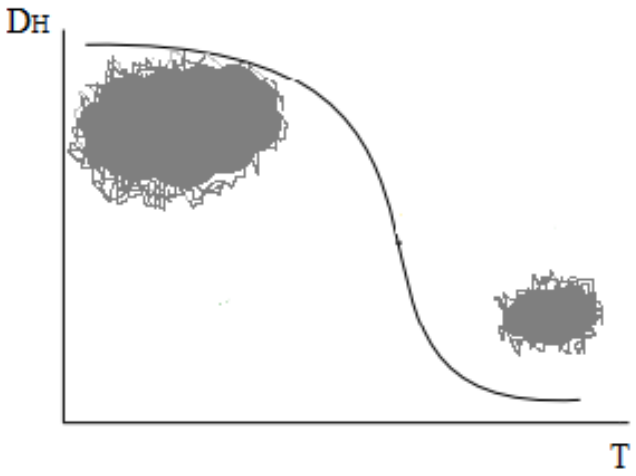

Figure 1.3. Below VPTT the PNIPAAm is water-swollen state, above VPTT PNIPAAm in collapse state

According to its temperature-sensitive swelling, this type of smart hydrogel can be classified into negatively temperature dependent hydrogels, and positively temperature dependent hydrogels. Negatively-temperature dependent hydrogels such as (PNIPAAm) with LCST collapses along with elevating the temperature. The polymer chains show soluble behavior at lower temperature, due to the dominance of the hydrogen bonds among water molecules and hydrophilic groups of polymer segments (dominant water-polymer interaction). However, with increasing the temperature the hydrophilic interaction among water molecules and polymer segments become weaker, whereas, the hydrophobic interaction among the hydrophobic groups in polymer chains become stronger, resulting in the deswelling of the gel and the collapse of polymer network (dominant polymer-

polymer interaction). Positively temperature-sensitive hydrogels with UCST show insoluble behavior at lower temperature, but once the temperature exceeds a certain value, the polymer chains display water-soluble behavior, thus the gel swells in water. **Table1** shows **LCST** of some hydrogels.

Hydrogel	LCST
Poly(N-isoprolylacrylamide), PNIPAAm	≈32
Poly(vinyl methyl ether), PVME	≈ 40
Poly(ethylene glycol), PEG	≈ 120
Poly(propylene glycol), PPG	≈ 50
Poly(methacrylic acid), PMAA	≈ 75
Methylcellulose, MC	≈ 80

Table2 LCST of some hydrogels in water [30].

Various thermo-sensitive polymers have been reported such as poly(N-alkyl substituted acrylamides), poly(N-vinylalkylamides), e.g. poly(N-vinylcaprolactam) and poly(N-isopropylacrylamide), respectively[28]. The most reviewed thermo-sensitive hydrogel is PNIPAAm, which has a sharp thermo-reversible LCST in aqueous solution, where the polymer chain morphology change from a random coil to globule [31]. PNIPAAm chains collapse at (32C) upon heating, but it swells reversible upon cooling [32]. With a lower critical solution temperature (LCST) close to temperature of the human body (37-36.5)C and excellent solubility in water, PNIPAAm is a perfect candidate in biomedical applications.

The LCST of PNIPAAm is determined by the interactions among water molecules and the polymer's functional groups, i.e. N-H, C=O present in the chemical structure of PNIPAAm as shown in **figure 1.4**

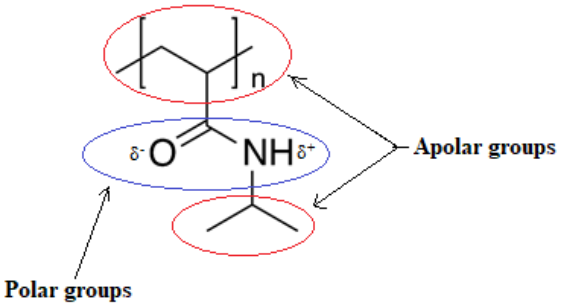

Figure 1.4 the chemical structure of PNIPAAm

Since it was first reviewed in 1968, PNIPAAm hydrogel have used in several applications, such as physics, astronomy, environmental science and biomedicine field the most explored subfields in biomedicine shown in **figure 1.5.**

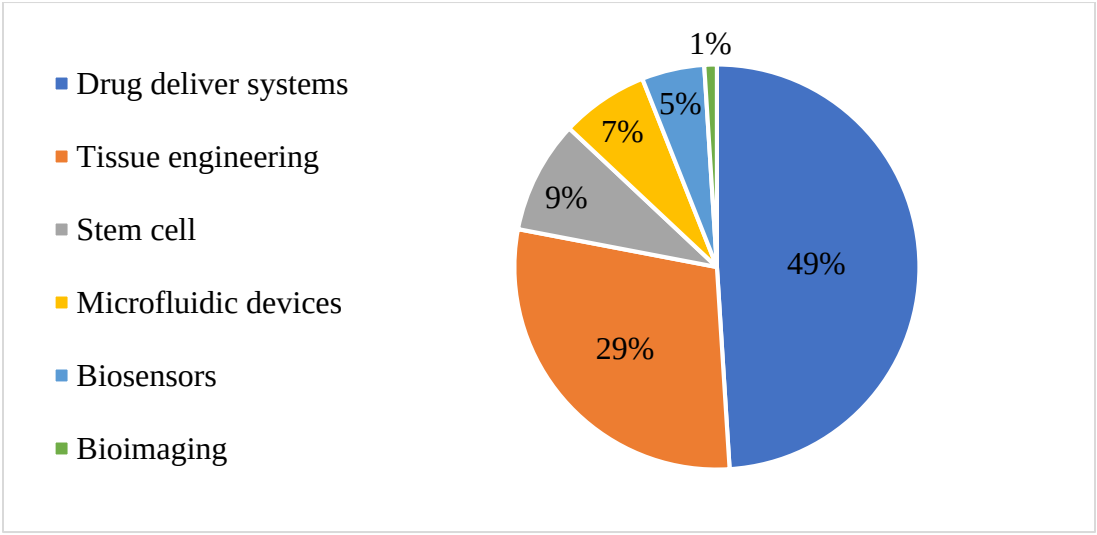

Figure 1.5. shows the percentage of PNIPAAm published research work in biomedicine field [32].

1.6.2 pH Responsive Hydrogel

Hydrogels containing basic or acidic ionizable groups such as carboxyl $-COOH$, amino $-NH_2$ and sulfonyl group $-SO_2$, are considered as pH-responsive hydrogels in which these groups are ionized by pH changes, that leads to conformation

changes of the polymer chains and to the changes in the properties of the hydrogels (hydrophilic/hydrophobic behavior, solubility, and volume). pH responsive hydrogels are important class of smart hydrogels that exhibit swelling or de-swelling behavior as a response to the change of the pH of the surrounding medium. In the recent years this class of smart hydrogels have been used widely in drug delivery system applications, as pH can vary between healthy and pathological body tissues as well as among tissues in the different organs, or among different compartments of the cells. For example, the stomach has to be an acidic medium while the pH of blood vessels is neutral, as we shall see later. Therefore, the importance of this class in delivery systems is to control the release of the cargo through their sensitivity to the change in the medium pH. pH responsiveness is due to the changes in the protonation of pendant ionizable groups present on the network of the polymer. Thus the rapid change in the charge density of the polymer leads to an alteration of the hydrodynamic volume of the polymer chains, while the osmotic pressure is not compensated by the elastic energy of the swollen polymer network [33].

Hydrogels with pH sensitivity can be either anionic with negative pendant groups or cationic with positive pendant groups.

Cationic Hydrogels

Cationic hydrogels have positively charged pendant groups such as amine. In this subclass the most important features are the pK_b of the polymer and the pH of surrounding medium. For example in a cationic hydrogel of amine groups, when the pH value of the surrounding medium is less than the pK_b, the charge of amine group alters from NH_2 to NH_3^+, leading to strong electrostatic repulsion in the gel network and swelling [34] [35]. In the next figures some examples are given for polybases.

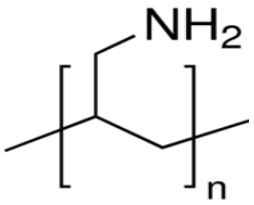

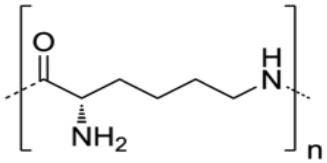

Poly(allylmine) Poly(ethylene imine) Poly(L-lysine)

- **Anionic Hydrogels**

Anionic hydrogels contain negatively charged pendant groups e.g. carboxylic or sulfonic acid groups. Anionic hydrogels with weak acidic groups are also pH responsive. If the surrounding medium pH is below the pK_a of the polymer the acidic groups are protonated. When the pH is increased above the pK_a the deprotonation of the acidic groups leads to increasing charge density and to the swelling of the gel network. [34,35]. The figure below shows some examples of polyacids.

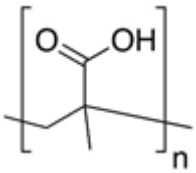

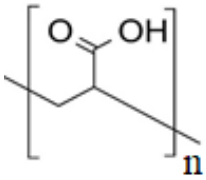

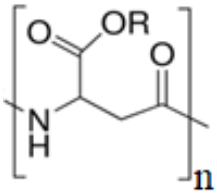

Poly(Methacrylic acid) Poly(acrylic acid) Poly(aspartic acid)

There are more classes of stimuli responsive hydrogel such as the electro-responsive hydrogel, magnetically responsive hydrogel and light responsive hydrogels but they are rarely used, thus, they had not discussed in this dissertation.

1.6.3 Dual-sensitive Hydrogels

Dual-sensitive hydrogels are a class of smart hydrogels that can simultaneously respond to more than one stimulus. In the biomedical field hydrogels are considered dual-sensitive if they show a theragnostic character which means they can be used in diagnostics and therapy simultaneously. This will support and increase the efficiency of the therapies. As an example, a polymeric material may give response to several types of stimuli while it can provide on-site diagnostics, while provides the cure by releasing its drug load.

One of the polymeric materials that possesses dual-responsive behavior is poly(N-isopropylacrylamide)-co-Allylamine hydrogel. This material is highly response to temperature and pH changes. Moreover, it is biocompatible. Therefore, poly(N-isopropyl acrylamide)-co-Allylamine is suitable in biomedical felid [28].

1.7 Recent Literature Reviews

Over the last few decays many papers have been published and presented novel hydrogels.

Several new synthetic and characterization methods as well as novel applications were proposed. Below I highlight two recent examples to demonstrate the potential unique applications of hydrogels.

1.7.1 Novel Applications of Hydrogels

Lu at el.[36] have reviewed a new development about the design, synthesis, properties and potential applications of electrophilic conductive hydrogels. Electroconductive hydrogels combine the properties of biomimetic feature of hydrogel and the electrochemical behavior of the conductive polymers. Due to their three-dimensional porous structure, electrochemical redox and hydrophilic

properties, they found that electroconductive hydrogels can be used to detect the electric signals given by biological systems, as well as supply the electrical stimulation to control the cell/tissue activity.

In another example [37] a thermo-sensitive hydrogel was prepared from amine-terminated poly(N-isopropylacrylamide). The polymer solution was added to a solution of $HAuCL_4$. The synthesized hydrogel (PNIPAAm/Au NPs) shows a sharp reversible transition at the LCST, which can be controlled by adjusting the molar ratio between $HAuCl_4$ and PNIPAm, as well as the reaction temperature. They demonstrated that at reaction temperature above LCST and higher PNIPAM concentrations drive the formation of larger Au NPs. The size range of the formed Au NPs was from 2 to 15 nm, which was determined by TEM, UV-Vis spectroscopy and SAXS/SANS.

1.7.2 PNIPAAm Microgels

There is no precise definition for microgels. Nevertheless, most of the aqueous microgels are cross-linked porous spherical particles with diameter that ranges between 10 nm to 50 μm. The most importantly microgels are highly swollen in the liquid phase, e.g. in water. Their degree of swelling depends on several parameters such as, pH, temperature and ionic strength of the liquid phase [38].

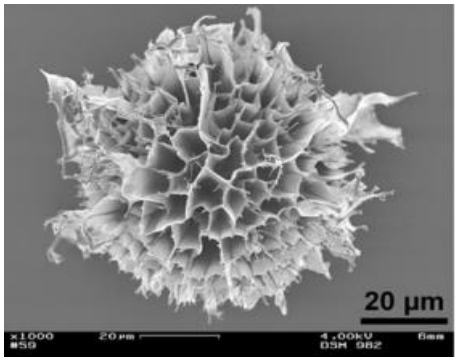

Figure 1.6. SEM image of PNIPAAm particle [38]

Microgels can be obtained by chemically or physically cross-linking. Various types of chemically crosslinked microgels can be formed, such as styrene [39], methyl methacrylate [40], N-isopropylacrylamide[41] microgels. The chemically cross-linked PNIPAAm microgels have a size that ranges from 30 to 1000 nm. They are typically obtained by free radical polymerization. After polymerization it is necessary purify them from excess monomers and oligomers, which is usually done by repeated centrifugation, decantation and redispersion [42].

In physically crosslinked microgels the network can be formed by hydrophobic forces, ionic interactions or H-bonds. Physical gelation can be affected by the ionic strength, concentration of the polymer, temperature and pH. For example, any changes in pH or increase the ionic strength the microgels probably will become colloidally unstable. Some examples of physically microgels are chitosan and alginate [43,44].

PNIPAAm microgel particles, which are usually crosslinked with methylenbisacrylamide (BIS), display VPTT. The VPTT is close to the physiological temperature. Furthermore, good colloid stability and control over monodisperse particle size makes PNIPAAm microgels very useful in different fields such as medicine [45], intelligent coatings [46] and biosensing [47].etc. The figure below shows the PNIPAAm microgel swelling/collapsing mechanism .

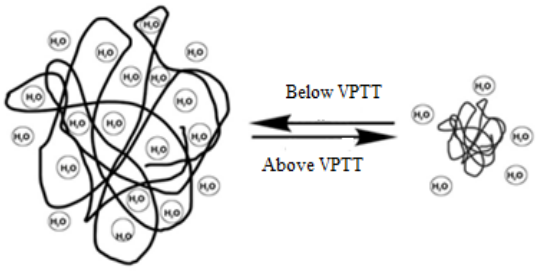

Figure 1.7. shows the swelling and collapsing mechanism of PNIPAAm microgels in water [48]

The crosslink density only slightly increases the VPTT of PNIPAAm microgels. At the same time, the relative swelling strongly depends on crosslink density. Microgels with high cross-link density are less swellable, and the VPT becomes more continuous due to the different polarity of BIS [49,50]. Various researchers studied the effect of addition of surfactants on the microgel particles size during the synthesis [46]. The type of surfactant has influence on the incorporation rate of acrylic acid, the size and the structure of the microgel particles, particularly at high concentration values of the surfactant. Using an anionic surfactant decreases the size and the incorporation rate of the acrylic acid, while a nonionic surfactants or cationic surfactants display the inverse behavior.

The chemical composition (copolymerization with different monomers), pH, the ionic strength influences the VPTT of PNIPAAm. A well-known principle is that the hydration degree of the polymer depends on the characteristic of the monomer units, thereby hydrophobic co-monomers decreases the value of VPTT whereas hydrophilic co-monomers increase the value of VPTT [51].

The composition of the aqueous medium can effect on the VPTT of the microgel. The less the polar cosolvent is added to water the higher the VPTT becomes. Ionic surfactants, for example, sodium dodecyl sulfate (SDS), may bind to the microgel above the critical aggregation concentration (cac). SDS binds to PNIPAAm to form a polymer/surfactant complex. This complex formation provides a polyelectrolyte nature to the microgel, increasing its swelling (hydrodynamic size) and the VPTT of the gel[52]. Salts can also affect the swelling of microgel particles. They are usually divided into two groups. The first group is the so-called *kosmtropic* group, which consists of strongly hydrated ions (CO_3^{-2}, SO_4^{-2} and HPO_4^{-2}). The second group is the so-called *chaotropes* includes (SCN^-, ClO_4^- *and* I^-), which are less hydrated. Generally, the existence of salt in

the medium will shift the LCST of the microgel, typically to a lower temperature Indeed, the effects of all parameters mentioned above can be detected experimentally [51,53].

1.7.3 Synthesis of PNIPAAm microgels

PNIPAAm microgels are usually prepared by precipitation polymerization, which is also known as dispersion polymerization. It is the most common technique used for the preparation of thermo-sensitive microgels. Precipitation polymerization is done by dissolving the monomer(s), crosslinker and initiator in water. The microgel particles are formed above the VPTT, at a particular temperature (50-70 C). The polymerization is initiated by the free radicals formed as the result of the decomposition of the initiator (peroxide or azo-based agent).

Many previous reports have been devoted to study the precipitation polymerization of PNIPAAm microgel. The first study in this regard was carried out by **Philip Chibante** in 1978 for preparation of PNIPAAm microgels. The next figure shows the mechanism for microgel preparation by precipitation technique [38].

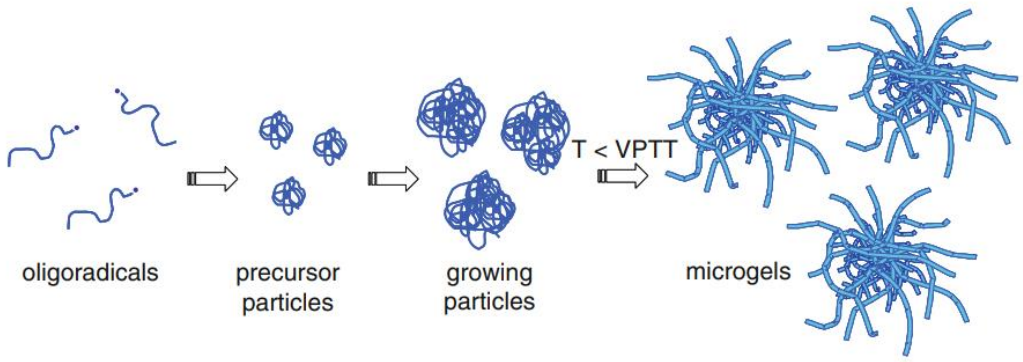

Figure 1.8. preparation of microgel by precipitation polymerization [38].

The radicals, which form by the decomposition of the initiator react with the water-soluble monomers and initiate the growth of the polymer chain (oligoradicals). However, the PNIPAAm chains become insoluble in water when they reach a critical length, thus they collapse. The collapsed growing PNIPAAm chains (precursor particles) aggregate with each other until the aggregate accumulates high enough surface charge to develop colloid stability. It should be noted that the surface charge of the growing microgel particles originates from the initiator and from the surfactant molecules that adsorb on the surface (e.g. SDS). An important characteristics of precipitation polymerization of PNIPAAm that it gives rise to monodispersed microgel particles, whose size can be controlled with the concentration of surfactants added to the reaction mixture.

Highly charged PNIPAAm microgels can also be prepared by precipitation polymerization if the functional co-monomer with anionic or cationic moieties is added to the reaction mixture. [54] These anionic or cationic moieties can shift the phase transition temperature, and they can be used as anchor site by interacting with other oppositely charged objects such as proteins or ions. According to the literature when allylamine is used as a co-monomer, PNIPAAm-co-Ala microgels with more than 10% allylamine content can be prepared.

1.7.4 Composite PNIPAAm microgels

Due to the unique structural properties, microgels can be used as microreactor, storage or carrier of various nano and sub-nanomaterials. Microgels offer an optimum reaction environment to synthesis various nanosized material inside the microgel structure. Several composite have been incorporated inside microgels such as noble metals [21], biominerals [55], metal oxides [56], and metal sulfides [57]. These composites do not change the stimuli sensitivity of microgels as well as maintain their physical or chemical behavior unchanged. In addition, by controlling the

swelling of the microgel the distance between the formed NPs can also be controlled. Moreover, NPs are stabilized within the microgel network. Nevertheless, high microgel loading with NPs can leads to undesirable interactions between the NPs and microgel network which can affect the mobility of the microgel chains as well as its swelling behavior.

Microgel loading with NPs is done by three approaches: (1) Microgels can be used as a microreactor to form the nanoparticles. For example, microgels have been used to synthesizing and stabilizing Pt NPs, the incorporated system of Pt within PNIPAAm used as a catalysis for different organic reactions [58]. In case of using the microgels as a reaction templates, the NPs are bound into the microgel network by hydrophobic interactions, hydrogen bonds or electrostatic forces. This approach is characterized by well-controlled NP dimensions as well as controlled NP loading. (2) In aqueous medium, microgels can be filled with NPs by diffusion. In this case the NPs can get entrapped within the microgel network by the electrostatic forces or by the hydrogen bonds. for example, a novel pH sensitive retinal/indocyanine green micelles as theragnostic incorporation used to treats the tumors [59]. This approach is widely used in drug delivery systems, where the drug adsorbed into microgel during the swelling state and released fast during the shrinking state. The drawback of this approach is that it is not suitable for inorganic nanocrystals prepared in organic medium. (3) This approach involves incorporation of NPs with reactive surface into the microgel network during the NPs preparation. In this case NPs get bound by covalent bonds. This approach allows high loading capacities, for example, a 3D hierarchical macro/mesoporous reduced graphene oxide anodes was fabricated in lithium-ion batters using poly(methyl methacrylate-co-glycidyl methacrylate-co-butyl acrylate) microgel spheres as a template [60 61].

1.8 Novel Fluorescent Probes

Since the 1990s, nanotechnology have attracted extensive scholarly attention in several research fields and nanoscale material such as quantum dots, carbon nanotubes, nanowires, metal nanoparticles and so forth have been widely investigated. One of the most important nonamaterial is gold nanoparticles (Au NPs) explored over 150 years when Michael Faraday observed that colloidal Au solutions and bulk Au behave differently. Later, it has been described that the color of Au NPs depends strongly upon the particles aggregation and the dimeter changes in the range between 10-100nm. Gustav Mie explained the color of Au NPs by realizing, when an incident light interacts with the free electrons in Au NPs it creates a collective oscillation of electrons known as localized surface plasmon resonance (LSPR). In contrast, particles with diameter less than 2 nm (ultrasmall particles) do not obey the LSPR excitation due to quantum size effect. These ultrasmall particles are called Nanoclusters (NCs). The size of NCs is closer to the Fermi wavelength of electrons, which leads to molecule-like properties such as discrete electronic structure with strong fluorescence in the visible and near inferred region. The unique optical and electronic properties, photostability, the high surface area to volume ratio, ease of surface functionalization to improve colloid stability made gold NCs popular candidates in several potential applications. In general, the surface functionalization is the key step for all Au NCs/NPs applications.

Xie at el, have developed a green synthetic rout to prepare BSA/Au complexes, at the physiological temperature of 37 C with red fluorescent under λ_{em} = 640nm [62]. They suggested that Au(III) ions were reduced and stabilized by BSA giving rise to red fluorescent gold nanoclusters built up by 25 Au atoms.

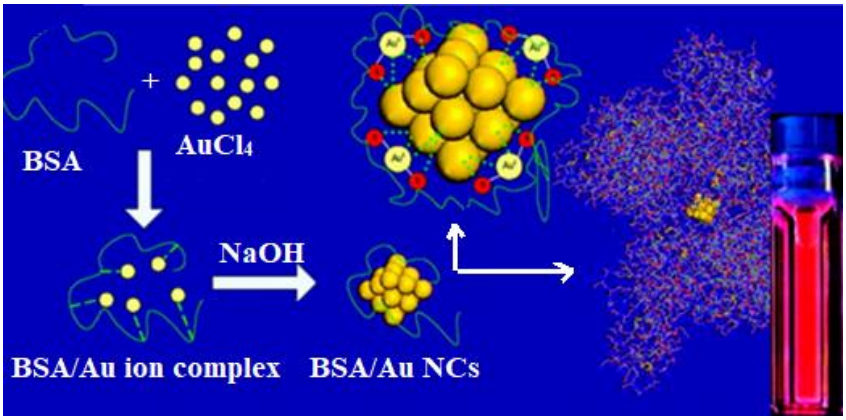

Figure 1.9. scheme represents formation of red fluorescence BSA/Au NCs complex

The authors have reported that, the optimization of reaction conditions is an important factor to obtain Au NCs with a highly quantum yield. For example, the reduction of Au ions occurred efficiently only at pH ~ 12. Another important factor was the reaction temperature. At 25 C the reaction ran very slowly and no Au NCs were obtained. However, reaction at the physiological temperature of 37 C Au NCs were obtained with high quantum yields within 12 hours, whereas, low quantum yield Au NCs were obtained when the reaction was conducted at 100 C. The third important factor was the concentration of BSA and Au precursors. When the BSA concentration was decreased at a fixed Au concentration relatively large NPs were formed which showed no fluorescence. The synthesis protocols are anticipated to be applicable for different types of proteins and noble metals[63].

Later **Dixon at el**, presented an alternative interpretation of the fluorescence of BSA/Au complexes[64]. They investigated the correlation between pH, BSA conformations and the fluorescence of the BSA/Au complex.

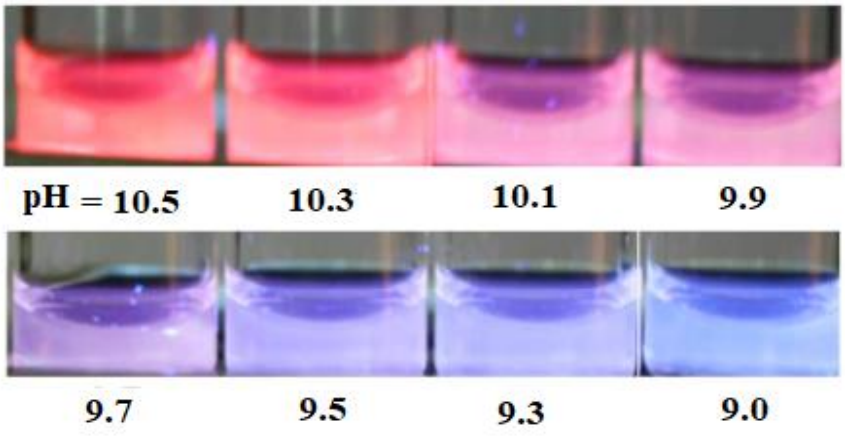

Figure 1.10. the red fluorescence (λ_{ex}=365 nm) of BSA/Au appears in aged conformation (pH > 10).

The red fluorescence of BSA/Au was connected to the Aged form (pH > 10) of the five-pH dependent BSA conformations. The rest of the BSA conformations expanding from pH <2.7, fast with 2.7<pH<4.3, normal with 4.3<pH<8, basic 8<pH<10 did not show red fluorescence. It was concluded that the red fluorescence of the BSA/Au complex is due to the binding of Au(III) ions on specific binding sites (on disulfide groups), which become accessible in the core of BSA in the open aged conformation of the protein. The red fluorescence was explained as the consequence of the energy transfer among the chromophores of the protein and the bound Au ions.

Varga at el. have investigated the effect of pH on the conformational state of BSA[65]. The investigations were carried out in the presence and absence of Au ions. First, they prepared two samples of BSA at pH = 7 and BSA/Au at pH = 7, denoted by BSA-7 and BSA/Au-7 respectively. Thus, they had two measurements categories:

- In the absence of Au ions.

BSA-7 (5.0%w) sample was prepared by Milli-Q water at room temperature, the stock solution diluted 10-fold either by water or NaOH to obtain BSA-12 stock solutions. A BSA-12 sample was heat treated for 2 hours at 37 C and then kept for two days at room temperature to obtain BSA-12HT. Finally, the pH of BSA-12HT was adjusted to 7 (BSA-7Re sample) and was kept for two days at room temperature. To investigate the effect of conformational changes on the fluorescence of BSA, the fluorescence of each sample was measured. The next table is to elucidate the fluorescence as a function of pH and conformation changes for the BSA sample in the absence of Au ions.

The sample	*The observation*
BSA-7	Blue fluorescence under $\lambda = 360$ nm was observed
BSA-12	Slight change in the fluorescence of BSA-7
BSA-12HT	Unchanged BSA-7 fluorescence
BSA-7Re	Increasing in the fluorescence was observed ($\approx 50\%$)

Therefore. the BSA conformation changes did not affect significantly the fluorescence of BSA in the absence of Au during pH cycle from 7 to 12 to 7.

- In the presence of Au ions.

A sample of BSA/Au (2.5%w / 5mM $HAuCl_4$) was prepared and diluted 5-fold with two different concentration of NaOH, to obtain BSA/Au-12 stock solution which was heat treated for 2 hours at 37 C and then kept for two days in the room temperature to obtain BSA-12HT. Then the pH of BSA-12HT was adjusted 7 again to obtain BSA/Au-7Re sample, which was also kept for two days at room temperature before its measurement.

The sample	*The observation*
BSA/Au-7	The blue fluorescence was detected, with a higher intensity than that of BSA-7
BSA/Au-12	The red fluorescence was detected.
BSA/Au-12HT	A negligible change in the in the red fluorescence
BSA/Au-7Re	A significant increase in red fluorescence (≈250%) was observed compared to BSA/Au-12, which was accompanied with decreasing blue fluorescence.

Varga at el. have also monitored BSA conformational changes by FTIR and SAXS during the pH cycle. They found that BSA did not regain fully its conformation after the 7 to 12 to 7 pH cycle. At the same time, it could be concluded that the red fluorescent species could form in the open conformation at pH=12 but when the pH was decreased the complex partially regained its more compact conformation at pH=7, which resulted in increasing red fluorescent.

Dissertation Layout

This dissertation is composed of three chapters. Chapter one provides above overview of the fundamentals of the hydrogels by reviewing their types, the preparation methods, the importance of the application of these systems and the possibility of using them in the medical and biological fields from the point of view of materials science. In chapter one also provide information and the main concepts related to PNIAAm microgels and the BSA/Au bioconjugate system. Chapter one ends with summarizing the objectives of the present dissertation.

Chapter two summarizes the experimental details of the work including the applied materials and the experimental methods adopted in the present research work. Finally the chapter ends with an overview of the instruments and characterization techniques.

Chapter three presents the results of my work and it is finished with a brief outlook of possible future research directions.

1.9 Objectives of The Present Investigation

The aim of my work was to investigate if the red fluorescent BSA/Au bioconjugate could be bound in high concentration in microgel particles to derive highly fluorescent soft nanoparticles with red emission for diagnostic purposes. Based on the above review, the synthesized PNIPAm-co-Ala copolymer have been used to associate with BSA/Au+ complex to exploit the fluorescence properties BSA/Au^{+} , BSA is define as a large molecular weight protein around 66.430 Da (583 amino acids) found in cow's circulatory system, also it a constituent of the whey component of bovine milk, the functional groups allows BSA to bind with fatty acids and other lipids probably by hydrophobic interactions, this feature is severely hampered upon denaturation[66].

- Preparation of PNIPAm-co-Ala based hydrogel.
- The study of swelling behavior of the synthesized hydrogel by evaluation the kinetic factors of the swelling/collapsing processes, also to study the effect of different parameters (pH, temperature) on the behavior of hydrogel by using DLs spectrometer, electrophoreses, UV light spectrophotometer.
- Preparation of BSA/Au bioconjugate complex system, then characterize the synthesized system of PNIPAm based hydrogel BSA/Au bioconjugate system by using the and fluorometer.

The general aim of the present research work is to provide a biocompatible theragnostic polymeric system of a well-controlled size and with the ability to use it as a diagnostic delivery system in the future, to increase the patient compliance, avoid the side effects as much as possible.

Previous work in the literature indicated that BSA binding was negligible in PNIPAm microgel particles at pH≥7. Since BSA is negatively charged

Chapter Two

2. Experimental section

This chapter deals with the starting materials and experimental techniques used in the present research work to impart the synthesis of poly (N-isopropylacrylamide)-co-Ala and preparation of BSA/Au complexes.

In this chapter the PNIPAAm-co-Ala, and BSA/Au samples preparation has been mentioned, characterization and testing methods are briefly reviewed as well.

2.1 *Materials*

N-isopropylacrylamide (NIPAAm), methylenbisacrylamide (BA), ammonium persulfate (APS) and sodium dodecyl sulfate (SDS) were purchased from Sigma-Aldrich.

N-isopropylacrylamide was recrystallized from hexane, methylenbisacrylamide was recrystallized from acetone and kept in a freezer, usually for a few days before they were used for the synthesis of the microgel particles. All other materials were used as received. All solutions were prepared in ultraclean Milli-Q water (total organic content = 4 ppb; resistivity = 18 mΩ·cm, filtered through a 0.2 μm membrane filter to remove particulate impurities).

2.2 Microgel Preparation

A precipitation polymerization technique was used to prepare poly(N-isopropylacrylamide-co-allylamine) microgels by copolymerizing allylamine that gives rise to the presence of primary amine groups in the microgel. Such microgels have positive charge below pH=10. The total concentration of the monomers was 130 mM in the reaction mixture, of which allylamine (ALa) was 13mM (10%), N, N-Methylene Bis-Acrylamide (BIS) was 1.86mM (crosslinker, crosslinking density

70 (130/70=1.86)), and the rest of the monomers was N-isopropylacrylamide (PNIPAAm), 115.14 mM. The reaction mixture also contained 0.3 mM cetyltrimethylammonium bromide (CTAB) stabilizer. The solution was introduced into a double-wall Pyrex glass reactor and it was stirred vigorously. To keep the temperature of the reaction mixture at constant 80 °C, the outer shell of the reactor was connected to a temperature bath and controlled temperature water was circulated in it. The reaction mixture was degassed by purging with nitrogen for 60 min. The synthesis was initiated with 2,2'-Azobis(2-methylpropionamidine) dihydrochloride (V50) initiator (0.6 mM). The synthesis lasted for 4 hours at 80 °C in nitrogen atmosphere.

To perform kinetic measurements, samples were taken from the reaction mixture as shown below:

1- 0min, 2- 1min, 3- 3min, 4- 5min, 5- 10min, 6- 20min, 7- 30min, 8- 45min, 9- 60min, 10- 90min, 11- 120min, 12- 240min, the samples were used to investigate the changes in the hydrodynamic particles size as a function of reaction time. The measurements were done both in an acidic medium (1mM HCl) and a basic medium (1 mM NaOH) at 25 and 40C. Moreover, the electrophoretic mobility of the microgels were also determined at a constant temperature (25 C).

The final microgel products were purified from unreacted monomers and polymeric byproducts by ultracentrifugation (Beckman Optima XPN ultracentrifuge, 362 000g, at 25 °C), decantation, and redispersion. The centrifuged microgels were redispersed in Milli-Q water and the cycle was repeated up to 3 times. The microgel concentration of in the purified microgel dispersion was determined by measuring the its dry mass and it was found to be 12.2 g/dm^3.

2.3 Dynamic light scattering (DLS)

Scattering is a feature of light when it hits molecules in solution which have a polarizability different from the surrounding medium. The oscillating dipole moment of the particles induced by the electric field of the incident light radiate in all directions. Dynamic light scattering, also known as photon correlation spectroscopy, provides information about the hydrodynamic size of particles suspended in the liquid phase. The information is gained by measuring the fluctuations of the scattered light intensity, the smaller particles move or diffuse rapidly, while the large particles move or diffuse slowly, thus the smaller particles give rise to faster fluctuations of the scattered light intensity while the larger ones result in slower fluctuations. The Brownian motion is a random movement of microscopic particles that originates from the collision between the particle and solvent molecules such as water. Since the light scattered by the different particles interfere at the detector the Brownian motion of the particles gives rise to a fluctuating scatting intensity at the detector. Taking into account that the rate of the Brownian motion is determined by the self-diffusion coefficient (D) of the particles, DLS measurements allow the determination of the D, which is usually converted to the hydrodynamic size by the Stokes-Einstein relationship assuming that the particles are spherical [67].

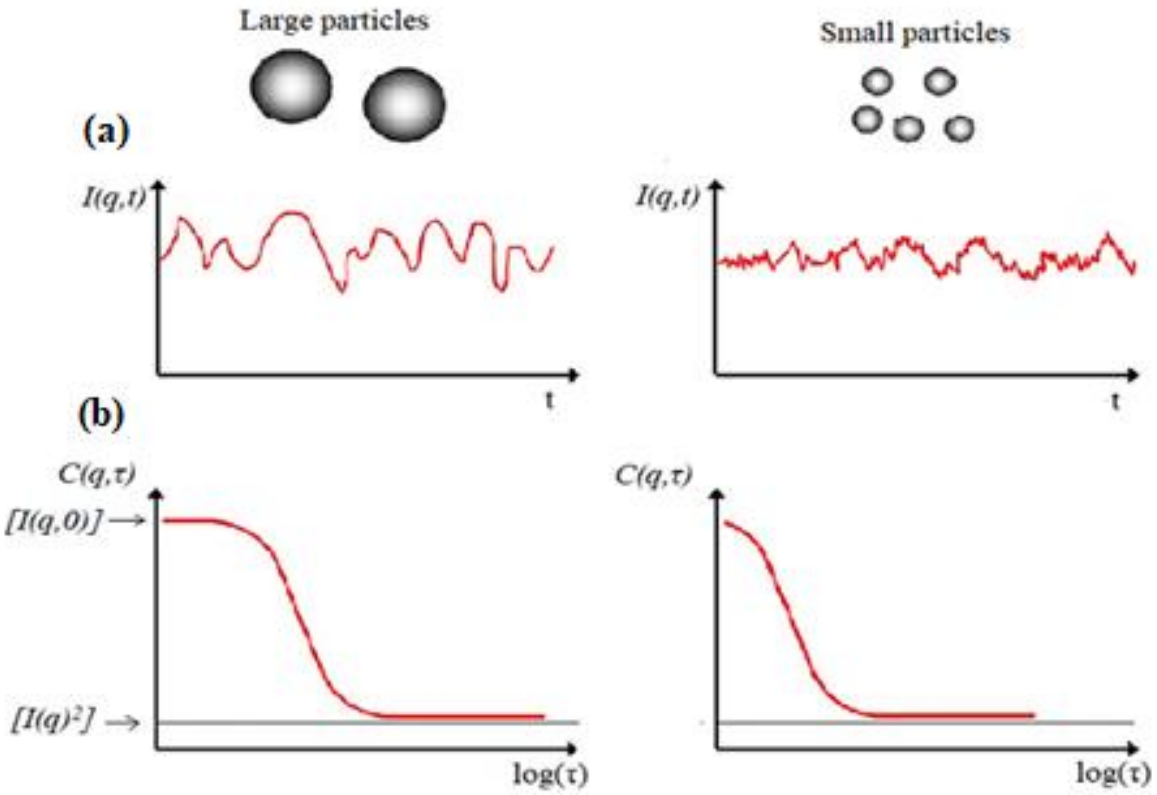

Figure 2.1 (a) shows the differences in intensity trace while (b) shows the differences in correlation function of large and small particles [68]

The correlation function is a mathematical translation of the fluctuations of the scattered light and describes how long a particle is located at the same spot within the sample. It is used to determine the translational diffusion coefficient (D). In the correlation function the intensity of the scattered light at a time (t) is compared to the same light intensity trace shifted by a delay time (τ) [68]. From this data, the correlation function, $g_2(\tau)$ can be determined. The decay rate Γ describes how fast the correlation function approaches zero. The relationship between the correlation function and Γ is shown below:

$$\sqrt{g_2(\tau) - 1} = Ae^{\Gamma\tau} \rightarrow (3)$$

Where A refers to an experimental coefficient, Γ is related to the scattering vector q and the diffusion coefficient D.

$$\Gamma = q^2 D \rightarrow (4)$$

From combining the equations above D coefficient can be calculated:

$$ln\sqrt{g_2(\tau) - 1} = lnA + q^2\tau \rightarrow (5)$$

From the equation above, the diffusion coefficient can be obtained by plotting $ln\sqrt{g_2(\tau) - 1}$ as function of τ, then D can be converted to the hydrodynamic size:

$$D = \frac{k_B T}{6\pi\eta r} \rightarrow (6)$$

where k_B is the Boltzmann's constant, T is the thermodynamic temperature and η refer to the solvent viscosity. The size provided by DLS is referred to as the equivalent hydrodynamic size, which is defined as the radius of the sphere that diffuses at the same rate as the particle being measured.

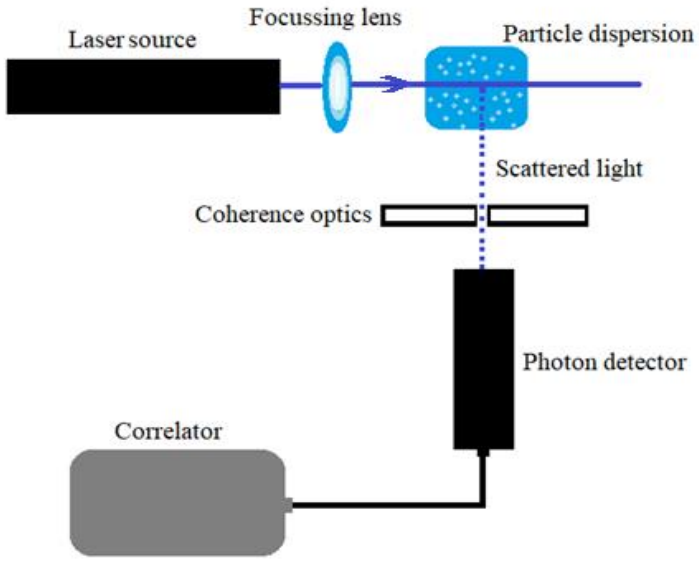

Figure 2.2 the optical circuit scheme of DLS instrument [69]

Figure 3.2 shows the main parts of a DLS instrument. The equipment contains a light source, which is usually a vertically polarized continuous laser in modern equipment. This shines light through the sample. The intensity of light scattered by a small volume element of the sample is measured at a fixed scattering angle by a photomultiplier, whose signal is fed into an autocorrelator. The autocorrelator is used to analyze the signal and determine the intensity-intensity autocorrelation function.

2.4 UV-Vis spectrophotometer

UV- Vis spectroscopy is one of the important analytical, optical techniques, which is used widely in the laboratories. In a UV-Vis measurement light in the visible (400 -800 nm) or ultraviolet (190 – 800 nm) range passes through a sample and its intensity is measured. The measured light is attenuated due to the absorption in the sample. The absorption can occur at a well-defined wavelength or over a wide spectral range.

UV-Vis spectrometry is a powerful characterization technique that provides information about electron transitions from the ground state to excited states. The energies of the orbitals involved in electronic transitions have constant values and that because of the quantization of molecular energy levels. Thus, the energy difference of the energy levels involved in the transition is also well-defined giving rise to the absorption peaks in the spectra. The width of the individual spectral lines can get rather large due to the large number of vibrational and rotational energy levels that are also involved in the excitation and due to the molecular interactions in the liquid phase. [70]

The scheme below shows the main units of a dual-beam UV-Vis spectrophotometer. The UV light is generated by discharge deuterium lamp while the visible light generated by a tungsten-halogen lamp. The instrument swaps the

lamps automatically as the wavelength is changed from the UV to the visible range. The light travels to a slit to increase focus. First the light beam is dispersed through a diffraction grating, then through a half-mirrored part, which splits the beam into two equal intensity beams, one of the separated beams named as the sample beam which travels through the sample, while the other one named as the reference beam which travels through the pure solvent. The absorption of the sample is determined by measuring the intensity of the sample and the reference beams by suitable detectors. The detectors could be photodiodes, phototubes or photomultipliers.

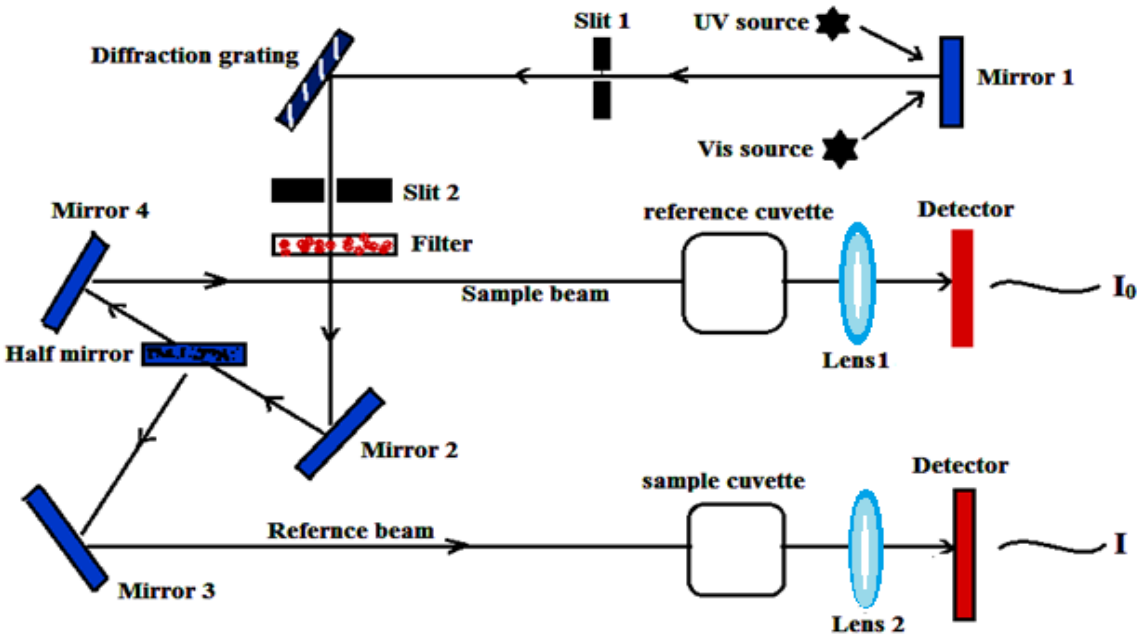

Figure 2.3 scheme of UV- Vis spectroscopy [71].

In the absence of sample (pure solvent) the light intensity leaving the sample cuvette (I), and the light intensity leaving the reference cuvette (I_o), will be the same: In this case the transmittance of sample ($T = \frac{I}{I_0}$) is 100%. When the sample absorbs light at a specific wavelength, the light intensity passing through the sample (I) is decreased, therefore, the transmittance decreases too.

Beer-Lambert found that "the absorbance of a solution is directly proportional to the concentration of the absorbing species in the solvent and to the optical path length":

$$A = -log\ (\frac{I_0}{I}) = \varepsilon.c.l \rightarrow (7)$$

Where *A* refers to Absorbance, I_0 is the initial intensity (references beam intensity), *I* is the transmitted intensity (sample beam intensity), *l* is the length of the light path through the cuvette, *c* is the concentration of the absorbing species and ε refers to molar Absorptivity [72].

2.5 Electrophoretic mobility measurement

Zetasizer is a powerful analytical instrument used for the measurement of the electrophoretic mobility (zeta potential) of small partnicles[73,74]. In an electric field the particles move toward the electrode of opposite charge. Once the electric force and the drag force acting on the particle becomes equal, the electrophoretic velocity of the particle become constant. Electrophoretic velocity $\vec{v}$ depends on the particle's radius, the viscosity of the medium and the force $\vec{F}$ of the electric field $\vec{E}$ as well.

$$\vec{v} = \frac{\vec{F}}{6\eta\pi R} \rightarrow (8)$$

The electrophoretic mobility is given by:

$$\mu = \frac{\vec{v}}{\vec{E}} \rightarrow (9)$$

In the case of an isolated particle, the force $\vec{F}$ originating from the electric field is equal to $q\vec{E}$, where the net charge on the microgel particles is q. Therefore, the electrophoretic mobility μ of a single particle is $\frac{q}{6\eta\pi R}$ [75].

A Malvern Zetasizer NanoZ instrument was used, which measures the electrophoretic mobility of the particles by laser Doppler velocimetry in combination with phase analysis light scattering (M3-PALS). This method allows the measurement of samples even with very low mobility. The standard error in the values of the electrophoretic mobility was around 10 %

2.6 Fluorometer

Fluorescence measurements are performed by using a spectrofluorometer. The optical modules of a fluorometer are the light source, a detector and three main units (Excitation module, Sample compartment, Emission module). The light source is usually a Xenon lamp (450W), which produces continuous irradiation of high-intensity light with a wide range of wavelengths typically from 250 to 700 nm. The excitation and emission modules (monochromators) consist of a series of gratings and mirrors to allow the independent selection of the excitation and emission wavelengths. In a normal measurement the sample is excited by the wavelength where it has an absorption maximum to allow the maximum number of excitations, and consequently to obtain the largest number of emitted photons from the sample. In the experiment part two distinct ways can be used. The first, by fixing, the excitation monochromator M1, and varies the emission monochromator M2 to obtains an emission spectrum. The emission spectrum can be obtained by comparing the measured intensity of the transmitted light (I) and comparing it to the measured wavelength of the transmitted light (λ_f) Alternately, emission monochromator M2 is fixed while the excitation monochromator M1 varied, this

yields an excitation spectrum. The excitation spectrum can be obtained by measuring the transmitted light intensity (I) and compare it to the measured wavelength of the incident light (λ_0) In the sample unit, the sample holder is adapted to measure the emitted light at an angle of 90°, which reaches the detector after travelling through the fluorescence monochromator that selects the measured emission wavelength [76,77].

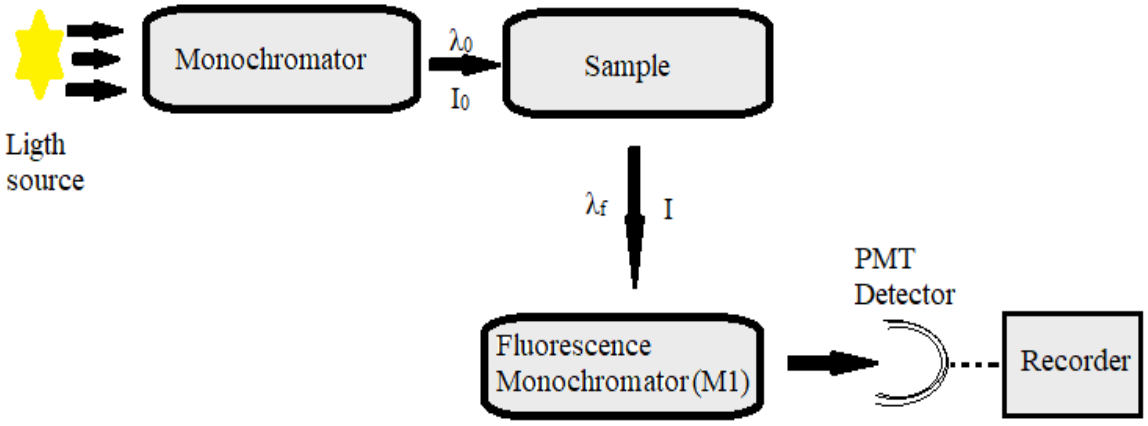

Figure 2.4 scheme of a basic spectrofluorometer

Fluorescent spectroscopy measurements were performed with a Jasco Spectrofluorometer FP-8300. The fluorescent spectra were recorded using 360 nm excitation and 5 nm slit widths in a 3x3 mm quartz cuvette.

Chapter Three

3 Results and disscoution

The aim of my work was to investigate if the red fluorescent BSA/Au complexes could be bound in high concentration in microgel particles to derive highly fluorescent soft biocompatible nanoparticles with red emission for diagnostic purposes. Unfortunately, literature investigations indicate that BSA has a negligible binding in PNIPAAm microgels above the isoelectric point of the protein (4.3). Since the BSA/Au bioconjugates have negative charge above the isoelectric point, to overcome the limited binding of BSA I aimed at preparing PNIPAm microgels with positive charges in the polymer network to facilitate the microgel / BSA interaction. Furthermore, since according to the literature allylamine can be readily copolymerized with NIPAAm, PNIPAAm-co-Ala microgel was prepared, which gives rise to the presence of primary amine groups in the microgel. Such microgels have positive charge below pH=10. Furthermore, the amine groups can also interact with the gold ions[79 65].

In the first part of this chapter, the experimental results have been presented concerning the synthesis of PNIPAAm-co-Ala microgel. The swelling and the electrophoretic properties of the prepared microgel are presented in the function of various parameters, such as temperature and pH. In the second part of the chapter the results about the microgel interaction with BSA, Au(III) ions and BSA/Au complexes are presented.

3.1 The synthesis and characterization of the PNIPAAm-co-Ala Microgel

The PNIPAAm-co-Ala microgel was prepared according to a widely used standard literature method. The allylamine content of the reaction mixture was chosen to

10%, while the crosslink density was 70 that is one in every 70 monomers was BIS. The reaction was initiated with V50 at 80 C and CTAB was used to control the size of the microgel particles. To monitor the growth of the microgel particles twelve samples were taken during the synthesis. The hydrodynamic size of the microgels in the unpurified kinetic samples were measured both at pH = 3 (in 1mM HC1) and at pH=11 (in 1mM NaOH). In both cases 50μl of PNIPAAm-co-Ala microgel of different reaction time were added to 10 ml aqueous HCl or NaOH solution. Therefore, the hydrodynamic size of the microgel particles in both acidic and basic aqueous solutions were investigated with a constant ionic strength. In the first case the amine groups in the microgel are protonated, thus polymer network is charged up, while in the second case the amine groups are deprotonated thus the microgel is uncharged. Measurements were done both at 25 C (swollen state) and 40 C (collapsed state) by using DLS instrument. **Figure 3.1** shows that, at the beginning of the reaction (0 minute) there were no microgel particles formed. Once the reaction was started (1 minute) the particles started to grow and then the microgel particles size increased dramatically until a particular point (to ≈ 20 minutes) where the hydrodynamic size became roughly constant.

The microgel particles measured at 25 C had larger hydrodynamic size compared to the samples measured at 40 C. This agrees with our expectation and reflects the swelling behavior of PNIPAAm microgels. Moreover, the samples measured in an acidic medium showed larger swelling compared to those measured in the basic medium.

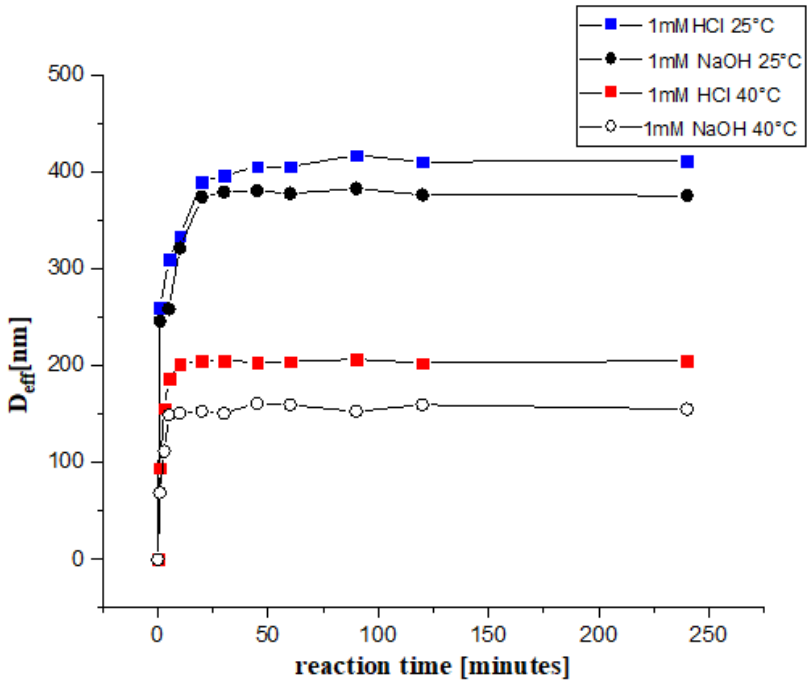

Figure 3.1 shows the hydrodynamic diameter of the microgel particles as function of the reaction time.

The larger hydrodynamic size in acidic medium relates to the dissociation constant (pK_a) of the Ala monomers, which is about 9.5. As a consequence, in a medium with pH larger than the pK_a of Ala, the particles are neutral, while they get protonated and charged up at lower pH. Thus, due to the presence of the charges the microgels swell in a larger extent giving rise to larger microgel hydrodynamic size.

3.2 The Evolution of the Electrophoretic Mobility of the PNIPAAm-co-Ala Microgel during the Particle Growth

The electrophoretic mobility of the kinetic samples was also investigated at 25 C both in the acidic and in the basic solutions. In the next figure, the relation between the reaction time and electrophoretic mobility is depicted.

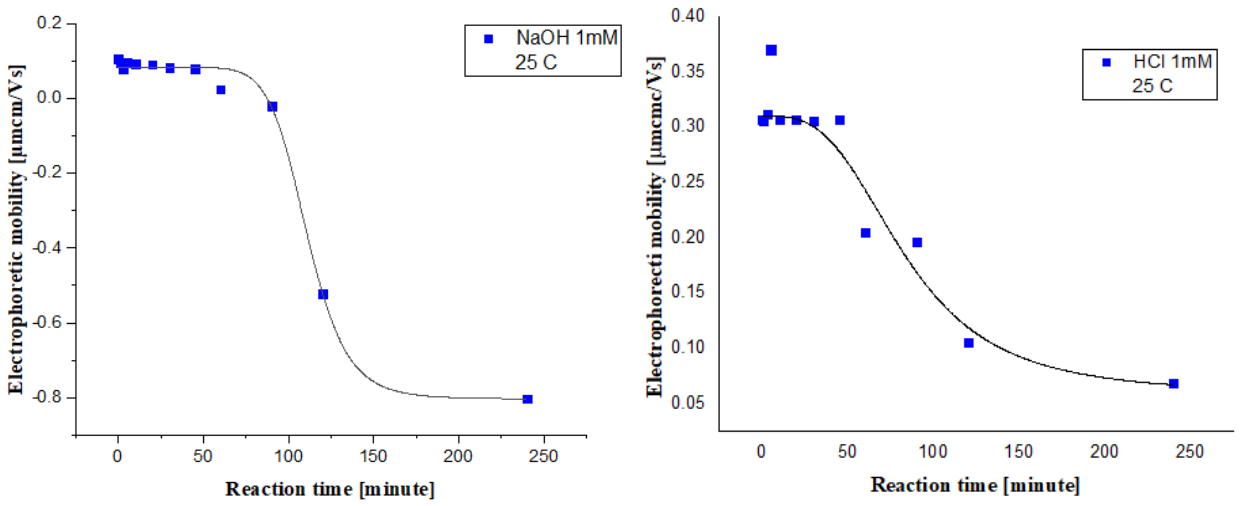

Figures 3.2 shows electrophoretic mobility of PNIPAAm-co-Ala at different reaction time

It is interesting to note that in the first ~50 minutes of the reaction the electrophoretic mobility stays a constant positive value both in acidic and basic environment. In the acidic solution the electrophoretic mobility is higher due to the protonation of the amine groups. At the same after 50 minutes the electrophoretic mobility starts to decrease. Since in this period of the reaction there is no significant particle growth this must reflect the decreasing surface charge. Indeed, in the basic solution the electrophoretic mobility shows a charge inversion. This may be rationalized in terms of chain transfer reactions that are known to generate negatively charged carboxylic groups on the polymer chains.

3.3 The effect of pH on the PNIPAAm-co-Ala Microgel

The final microgel particles were purified by repeated centrifugation, decantation and redispersion in water using a Beckmann ultracentrifuge (362 000 g at 25 C). After the third centrifugation cycle the microgel was lyophilized. All further

experiments were carried out by using an aqueous microgel stock solution (12.25 g/dm^3) prepared from the lyophilized sample.

A set of PNIPAAm-co-Ala samples were prepared at different pH values and constant ionic strength at 25 C. The hydrodynamic size of the final purified microgels was measured by dynamic light scattering.

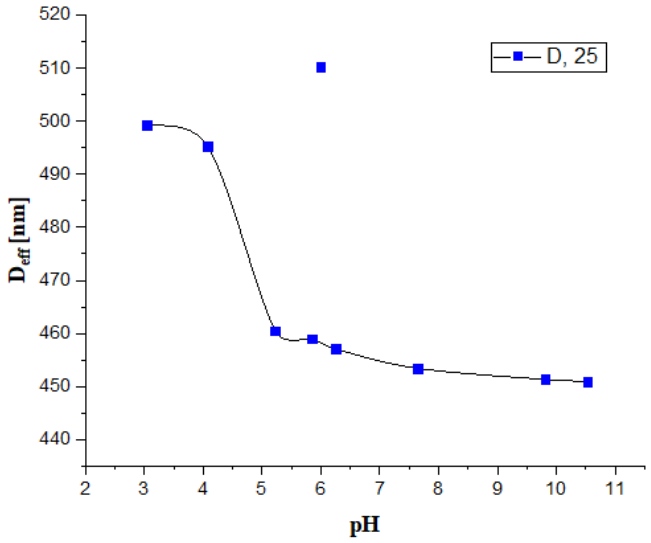

Figure 3.3 the change in Hydrodynamic particles size at different pH values.

The variation in hydrodynamic size of PNIPAAm-co-Ala microgels was investigated at constant ionic strength of (1mM NaCl). At lower pH values, the PNIPAAm-co-Ala microgel particles have a larger hydrodynamic size. This is due to the presence of the protonated amine groups. This result agrees qualitatively with those in the **figure 3.1**, though the measured absolute values are somewhat smaller for the purified sample indicating the loss of uncross-linked chains from the microgel particles.

The electrophoretic mobility of the microgel particles was also measured at 25 C as a function of the solution pH. The results are plotted in **figure 3.4.**

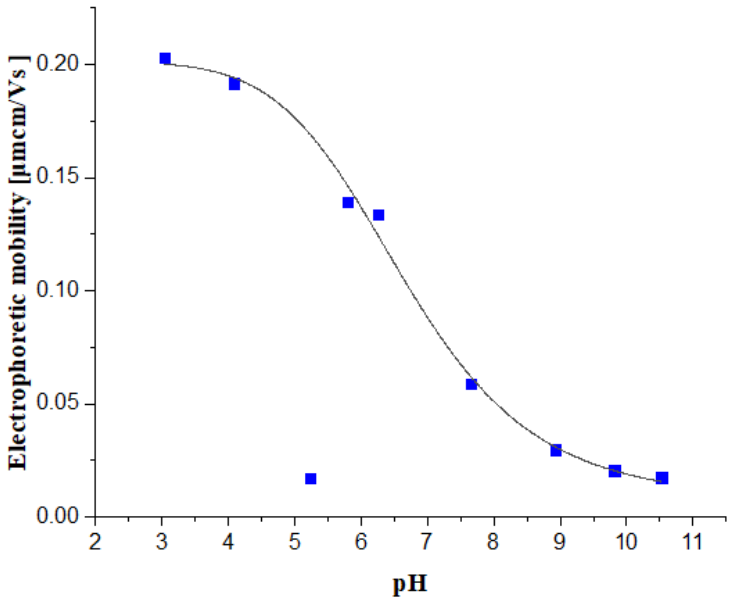

Figure 3.4 shows the effect of the pH changes on the electrophoretic mobility of the microgel particles.

Interestingly, in this case the electrophoretic mobility remains positive in the entire pH range, which seems to be in contradiction with the results measured on the kinetic samples. However, it should be noted that these results resemble the kinetic data after ~50 minutes reaction time after which the electrophoretic mobility sharply decreased for the kinetic samples. Further, DLS data on the purified sample showed loss of material due to the purification. This implies that in the final stage of the reaction PNIPAAm chains generated in the bulk and gained negative charge due to chain transfer reactions were attached by the electrostatic interaction to the microgel surface. However, due to the purification these non-crosslinked oligomers could be removed revealing the positive surface charge of the microgels.

3.4 The Temperature-dependent swelling of the PNIPAAm-co-Ala microgel

Finally, the hydrodynamic sizes of the PNIPAAm-co-Ala microgel was measured as a function of temperature from 25 to 50 C in the acidic solution (pH=3). The sample undergoes completely the VPT at 32.84 C. Taking into account that the uncharged PNIPAAm microgel has a VPTT at 32 C, and it is expected that charges incorporated in the polymer network increase the VPTT, this is a rather surprising results, which seems to indicate that PNIPAAm-co-Ala microgels contain only a limited amount allylamine copolymerized into the gel network. At the same time comparing the temperature dependent swelling of the microgel prepared in this work with the literature result, it can be concluded that these results are in good agreement with those presented in the literature [80].

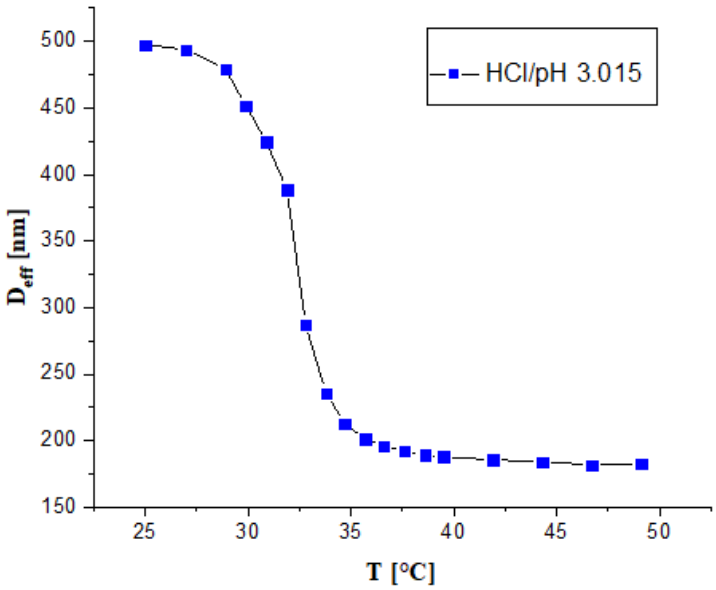

Figure 3.5 the swelling curve of PNIPAAm-co-Ala as a function of temperature

3.5 Investigation of the binding of BSA, Au(III) and BSA/Au in PNIPAAm-co-Ala microgel

To investigate the binding possibility of BSA within the microgel, a negatively charged BSA solution (150 µl, 5 w%, pH~7) was added to a positively charged PNIPAAm-co-Ala (750 µl, 1.22 w%, pH~7). They were mixed with 600 µl Phosphate buffer of different pH values to set the final pH of the mixtures and stored overnight at room temperature. To measure the binding of BSA on the microgel particles, the microgels were separated from the equilibrium solution by centrifugation and the BSA concentration was determined in the supernatant solution by UV spectrometry. For this purpose a BSA concentration calibration curve was determined using the absorption peak of BSA at 278 nm (**Figure 3.6**).

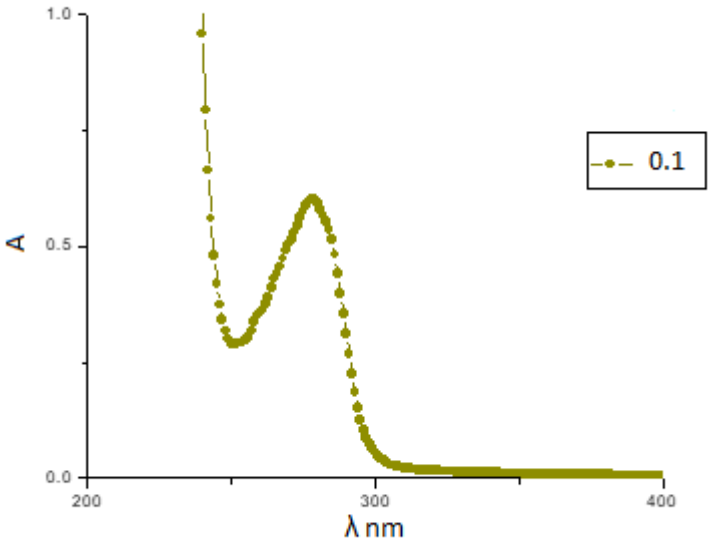

Figure 3.6 shows the BSA absorbance with different concentration and the corresponding wavelength

Since, despite their purification microgel solutions usually leak some oligomers during their storage, I also checked if the supernatant of a concentrated (1.25 w%)

pure microgel solution has any absorption at 278 nm. As it is indicated in **figure 3.7** a small absorption can be indeed observed. This contribution to the absorption of the supernatants was taken into account during the BSA concentration measurements.

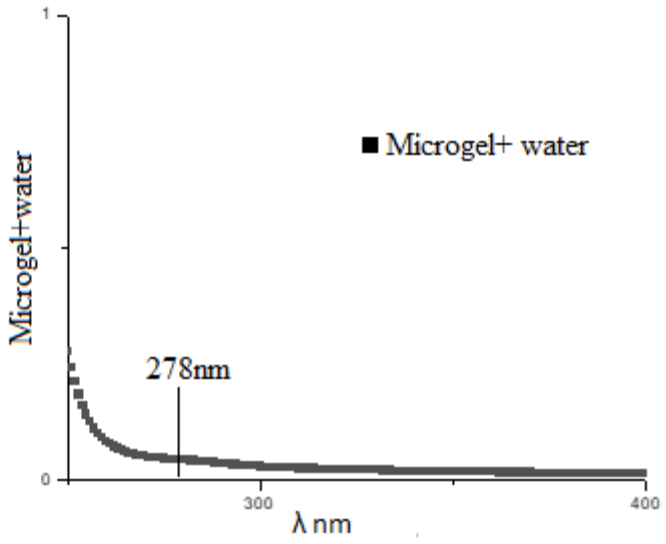

Figure 3.7 Absorbance curve of supernatant of PNIPAAm-co-Ala

The binding of BSA on the microgel particles was determined as the difference of the initial BSA concentration added to the solution and the equilibrium BSA concentration measured in the supernatant:

$$c_{Bound,BSA} = c_{0,BSA} - c_{eq,BSA}$$

The concentration of the microgel bound BSA, as well as its initial and equilibrium concentration is plotted in **figure 3.8** as function of the pH. Despite the opposite charges of BSA and the PNIPAAm-co-Ala microgel the initial and the equilibrium concentration of BSA is practically identical in the samples regardless of the pH, which indicates that the BSA binding is practically zero on the microgel.

The reason behind this unexpected result can be that, either the PNIPAAm-co-Ala microgel have less amine groups copolymerized in the chain than implied by the literature results or the positive charges are localized in the core of the microgel particles, which is surrounded by a densely cross-linked PNIPAAm shell, which could block the transport of the protein to the charged core.

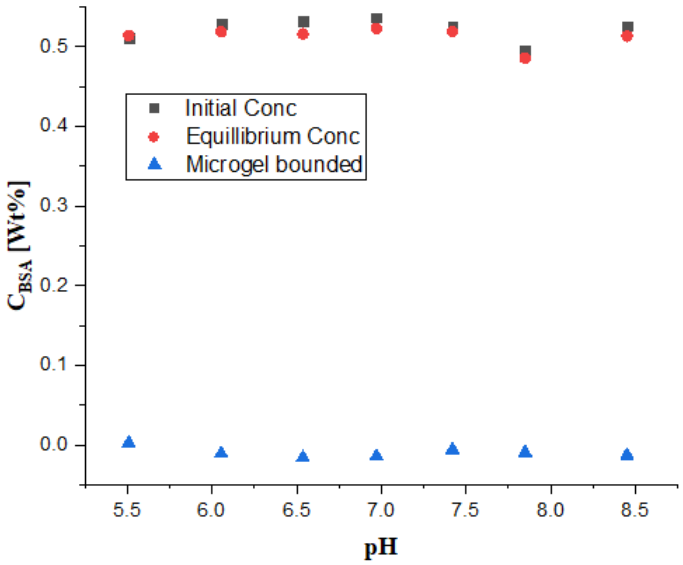

Figure 3.8 the BSA binding within Microgel

As a next step the binding of Au(III) to the PNIPAAm-co-Ala microgel was investigated. In this case the access of the small Au(III) ions to the amine groups should not be blocked even if they are localized in a core of a highly crosslinked PNIPAAm shell. To investigate the binding between Au(III) and PNIPAAm-co-Ala, first a series of samples have been prepared without any pH adjustment. The samples contained Au(III) in different concentrations and the same microgel concentration was used as previously in the case of BSA binding measurements. To measure the binding of Au(III) on the amine groups present in the microgel particles, the microgels were separated from the equilibrium solution by

centrifugation and the Au(III) concentration was determined in the supernatant solution by UV spectrometry at fixed a fixed pH=3. For this purpose a Au(III) concentration calibration curve was determined using the absorption peak of Au(III) at 227 nm (**Figure 3.9**).

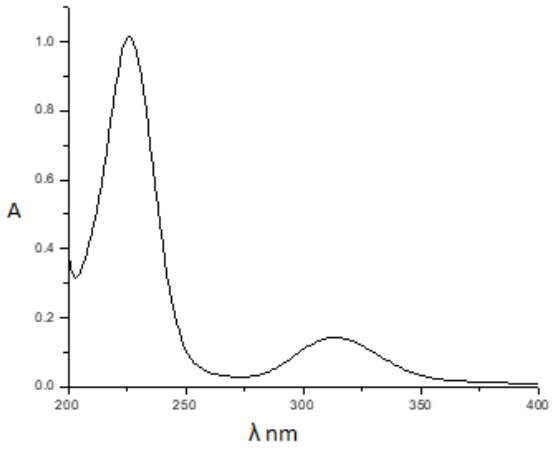

Figure 3.9 Absorbance curve of supernatant of PNIPAAm-co-Ala

The Au(III) ions are expected to bind on the amine groups of PNIPAAm-co-Ala. In the figure below the curve of the binding between PNIPAAm-co-Ala and Au(III), start from the zero then rise up steeply until reach ~0.22 mM Au(III) concentration. In this range the bound amount and the initial Au(III) concentration are almost equal with each other, which indicates very low equilibrium Au(III) concentration that is almost stoichiometric binding. At the same time above ~0.22mM Au(III) concentration, the binding reaches saturation implying that no more amine groups are available for gold binding. This result confirms that the prepared microgel contains orders of magnitude less amine groups then expected from the composition of the reaction mixture (~10 mM).

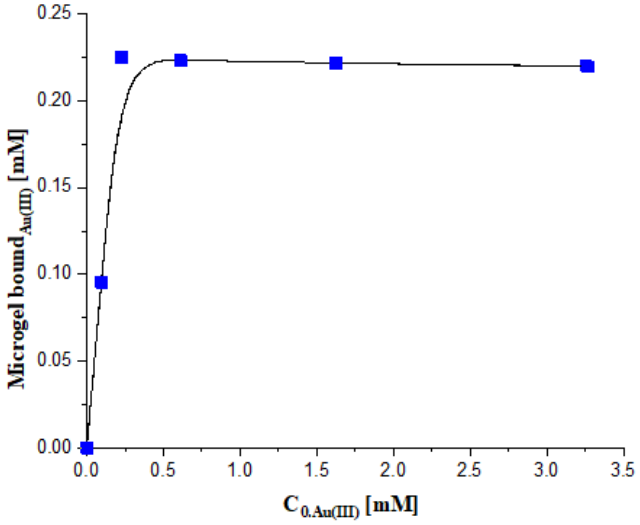

Figure 3.10 shows the Au(III)/PNIPAAm-co-Ala binding process

I also tested Au(III) binding on PNIPAAm-co-Ala microgels that had pH = 12 set before the mixing with $HAuCl_4$ solution. Different concentration of Au(III) solutions were used, while the microgel concentration was kept constant as in the previous experiments. Due to the acidic pH of $HAuCl_4$ the pH of the final mixtures varied in a wide pH range (from 2.9 to 11.3). The samples were stored at room temperature for two days. Pictures were taken of the fresh mixtures **(figure 3.11)**, then after one day **(figure 3.12)** and two days **(figure 3.13)**.

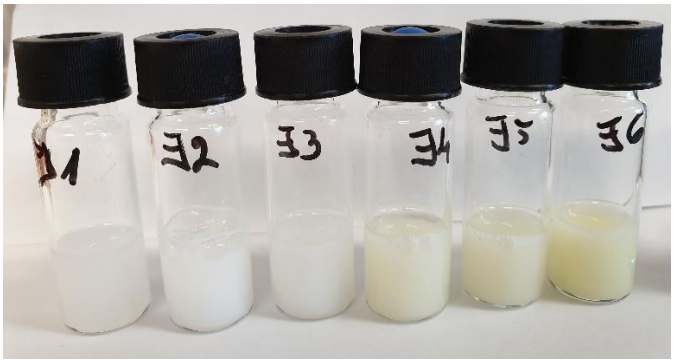

Figure 3.11 shows the fresh samples of PNIPAAm-co-Ala/Au(III)

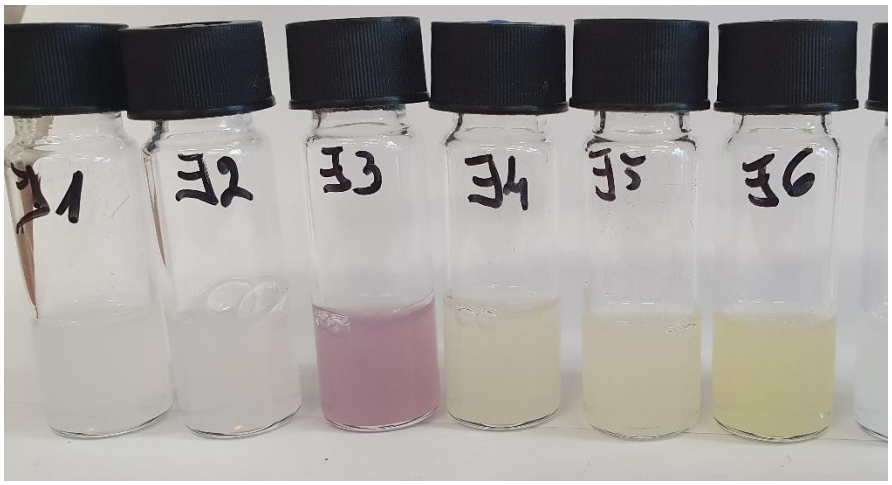

Figure 3.12 shows the BSA/Au bioconjugate /PNIPAAm-co-Ala samples in water after one days from preparation

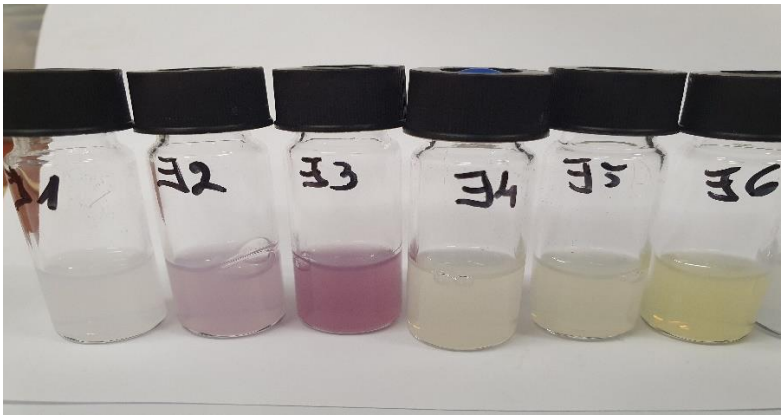

Figure 3.13 shows the BSA/Au bioconjugate /PNIPAAm-co-Ala samples in water after two days from preparation

As its is indicated by the figures after one day the third sample ($c_{Au(III)}$= 0.4 mM, pH=10.7), then after two days the second sample ($c_{Au(III)}$= 0.2 mM, pH=11.2) has also turned purple. The 4th, 5th and 6th samples have acidic pH (3.7, 3.5, 3.0), thus they did not turn purple despite of their higher Au(III) concentrations (0.8, 1.6 and 3.2 mM, respectively). The observed purple color is typical for plasmonic Au NPs, thus we can conclude that at high pH the amine groups of the microgels can reduce

the gold ions present in the solution, which presumably leads to the formation of microgel bound gold nanoparticles.

Finally the binding of the red fluorescent BSA/Au bioconjugate to the microgel was tested. Since at pH=12 the formation of plasmonic nanoparticles was observed in the microgel / Au(III)-ion mixtures, in this case the red fluorescent bioconjugate was prepared first then its pH was decreased to pH = 7 – 8 before mixing it to the microgel. This could be done because it has already been established that the red fluorescence of BSA/Au bioconjugates is preserved at pH=7 once it has developed at high pH. Namely 5 w% BSA solution was mixed with 10 mM HAuCl4 solution in equal volumes. Then the solution pH was set to ~12 and the mixture was heat treated for two hours at 37 C. After the heat treatment the mixture was stored at room temperature for two days. During this time it developed red fluorescence.The fluorescent spectrum of BSA/Au bioconjugate is plotted in **figure 14**.

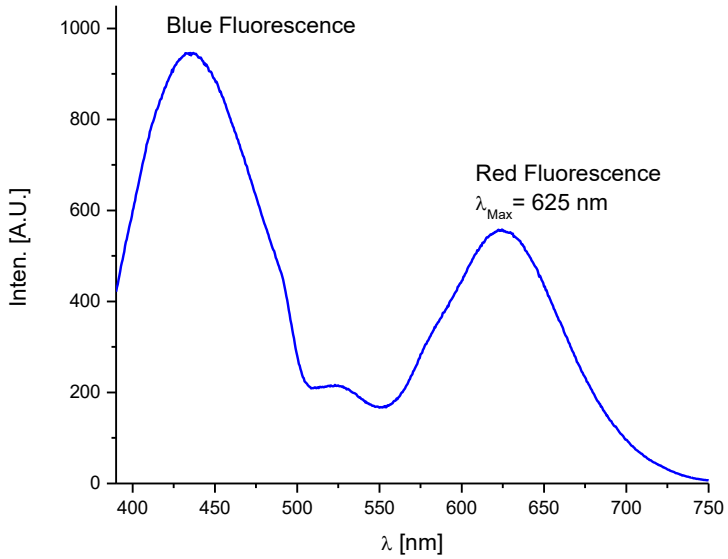

Figure 3.14 shows the fluorescent spectrum of BSA/Au bioconjugate.

A concentration series of the BSA/Au bioconjugate was prepared and mixed with equal volume of microgel solutions. The final samples had a constant 0.6 w% microgel concentration and the BSA concentration was varied from 0.1 to 0.4 w%. The prepared mixtures were stored at room temperature for one day (**figure 15**).

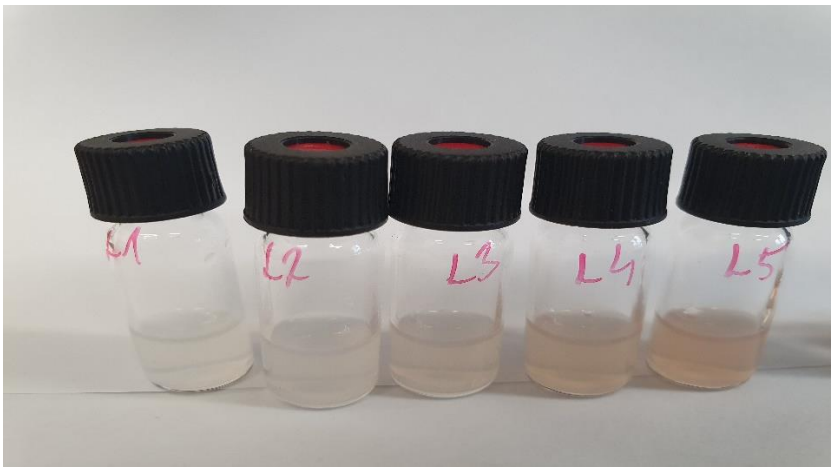

Figure 3.15 the BSA/Au bioconjugate PNIPAAm-co-Ala samples after one day from preparation

Finally, the microgel particles were centrifuged and the fluorescent spectra of the supernatant were measured for each sample. As a reference the fluorescent spectra of the microgel free BSA/Au concentration series was also determined. In **figure 3.16** the fluorescent intensities measured for the supernatants at 625 nm and normalized by the fluorescent intensities determined for the equal BSA concentration but microgel free BSA/Au samples are plotted. In this graph the value of one indicates that the supernatant has the fluorescent intensity expected due to the dilution of the BSA/Au bioconjugate. However, as it is shown by the figure the fluorescent intensity is slightly but significantly lower than one for each sample indicating a small amount of BSA/Au bioconjugate binding to the microgel.

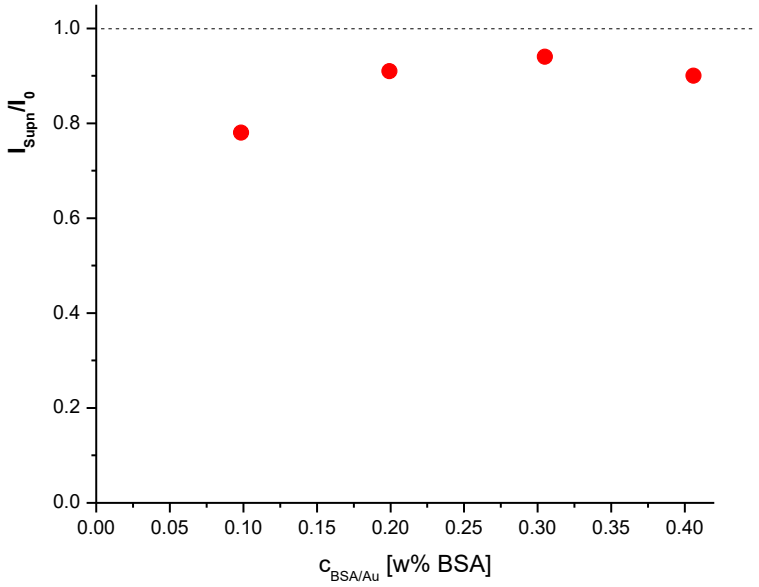

Figure 3.16 the BSA/Au red fluorescence normalized to the BSA concentration as a function BSA concentration in the PNIPAAm-co-Ala samples

These results imply that if microgel particles with significantly higher amine content could be prepared significantly more, red fluorescent BSA/Au bioconjugate could be bound in the microgels resulting in the desired red fluorescent microgels. The enhanced binding of the BSA/Au bioconjugate compared to the binding of BSA is presumably due to the presence of gold ions bound to the exterior of protein, which can facilitate the binding of the complex to the amine groups of the microgel.

Conclusion

In summary, thermosensitive microgels exhibit a unique swelling behavior as a result of the changes in the external stimuli, where the network structure swell or collapse at a certain transitional temperature. Among them PNIPAAm-co-Ala microgel have drown much attention especially in the medical and biological fields. Herein, positively charged PNIPAAm-co-Ala has been prepared by precipitation polymerization. Allylamine was aimed at co-polymerizing into the polymer network to facilitate the binding of negatively charged BSA/Au bioconjugates within the positively charged microgel. The microgel formation, as well as the swelling and charged nature of the microgel was investigated by Dynamic light scattering (DLS) and electrophoretic mobility measurements.

In the second part of my work the interaction of the prepared PNIPAAm-co-Ala microgel with Bovine Serum Albumin (BSA), Au(III) ions ($HAuCl_4$) and BSA/Au bioconjugate was investigated. The effect of the medium pH on the BSA binding to the microgel was investigated first. Despite of the electrostatic force between the positively charged PNIPAAm-co-Ala and the negatively charged BSA, the results shown no interaction between PNIPAAm-co-Ala and BSA. On the other hand Au(III) ions were entrapped into PNIPAAm-co-Ala microgel but the binding went to saturation at 0.22 mM Au(III) concentration, which implies that the amine concentration of the microgel network is much lower than expected from the composition of the reaction mixture. It was also found that when the PNIPAAm-co-Ala microgel / Au(III) ion mixture has a basic pH then the gold ions are reduced by the amine groups present in the microgel resulting in the formation of plasmonic nanoparticles.

Finally, the binding of the red fluorescent BSA/ bioconjugate was investigated in the PNIPAAm-co-Ala microgels at pH ó 7 - 8. A small but significant binding of the bioconjugate could be observed, which imply the important role of the BSA bound gold ions in enhancing the protein binding. These results also imply if microgels with significantly higher amine grafting could be prepared the BSA/Au bioconjugate binding could be significantly enhanced in the microgel.

SUMMARY

Investigation of BSA/gold bioconjugate/poly(N-isoprylacrylamide) microgel interaction

MAZIN ALI, MSc student in Materials Science

Place of diploma work: Department of Physical Chemistry, Institute of Chemistry, Eötvös Loránd University, Budapest

Place of defense: Department of Physical Chemistry

Supervisor: **Dr. Imre Varga**, associate professor
Department of Physical Chemistry

In summary, thermosensitive microgels exhibit a unique swelling behavior as a result of the changes in the external stimuli, where the network structure swell or collapse at a certain transitional temperature. Among them PNIPAAm-co-Ala microgel have drown much attention especially in the medical and biological fields. Herein, positively charged PNIPAAm-co-Ala has been prepared by precipitation polymerization. Allylamine was aimed at co-polymerizing into the polymer network to facilitate the binding of negatively charged BSA/Au bioconjugates within the positively charged microgel. The microgel formation, as well as the swelling and charged nature of the microgel was investigated by Dynamic light scattering (DLS) and electrophoretic mobility measurements.

In the second part of my work the interaction of the prepared PNIPAAm-co-Ala microgel with Bovine Serum Albumin (BSA), Au(III) ions (HAuCl4) and BSA/Au bioconjugate was investigated. The effect of the medium pH on the BSA binding to the microgel was investigated first. Despite of the electrostatic force between the positively charged PNIPAAm-co-Ala and the negatively charged BSA, the results shown no interaction between PNIPAAm-co-Ala and BSA. On the other hand, Au(III) ions were entrapped into PNIPAAm-co-Ala microgel but the binding went to saturation at 0.22 mM Au(III) concentration, which implies that the amine concentration of the microgel network is much lower than expected from the composition of the reaction mixture. It was also found that when the PNIPAAm-co-Ala microgel / Au(III) ion mixture has a basic pH then the gold ions are reduced by the amine groups present in the microgel resulting in the formation of plasmonic nanoparticles.

Finally, the binding of the red fluorescent BSA/ bioconjugate was investigated in the PNIPAAm-co-Ala microgels at pH ó 7 - 8. A small but significant binding of the bioconjugate could be observed, which imply the important role of the BSA bound gold ions in enhancing the protein binding. These results also imply if microgels with significantly higher amine grafting could be prepared the BSA/Au bioconjugate binding could be significantly enhanced in the microgel.

References

(1) Boulaiz, H.; Alvarez, P. J.; Ramirez, A.; Marchal, J. A.; Prados, J.; Rodríguez-Serrano, F.; Perán, M.; Melguizo, C.; Aranega, A. J. I. j. o. m. s. Nanomedicine: application areas and development prospects. **2011**, *12*, 3303-3321.

(2) Wallace, G. G.; Teasdale, P. R.; Spinks, G. M.; Kane-Maguire, L. A.: *Conductive electroactive polymers: intelligent polymer systems*; CRC press, 2008.

(3) Koltzenburg, S.; Maskos, M.; Nuyken, O.: *Polymer Chemistry*; Springer, 2017.

(4) Kamaly, N.; Yameen, B.; Wu, J.; Farokhzad, O. C. J. C. r. Degradable controlled-release polymers and polymeric nanoparticles: mechanisms of controlling drug release. *J Chemical reviews* **2016**, *116*, 2602-2663.

(5) Wichterle, O.; Lim, D. J. N. Hydrophilic gels for biological use. *J Nature* **1960**, *185*, 117-118.

(6) Fu, R.; Tu, L.; Zhou, Y.; Fan, L.; Zhang, F.; Wang, Z.; Xing, J.; Chen, D.; Deng, C.; Tan, G. J. C. o. M. A Tough and Self-Powered Hydrogel for Artificial Skin. *J Chemistry of Materials* **2019**, *31*, 9850-9860.

(7) Hakkarainen, T.; Koivuniemi, R.; Kosonen, M.; Escobedo-Lucea, C.; Sanz-Garcia, A.; Vuola, J.; Valtonen, J.; Tammela, P.; Mäkitie, A.; Luukko, K. J. J. o. C. R. Nanofibrillar cellulose wound dressing in skin graft donor site treatment. *J Journal of Controlled Release* **2016**, *244*, 292-301.

(8) Boulaiz, H.; Alvarez, P. J.; Ramirez, A.; Marchal, J. A.; Prados, J.; Rodríguez-Serrano, F.; Perán, M.; Melguizo, C.; Aranega, A. J. I. j. o. m. s. Nanomedicine: application areas and development prospects. *J International journal of molecular sciences* **2011**, *12*, 3303-3321.

(9) Chirani, N.; Gritsch, L.; Motta, F. L.; Fare, S. J. J. o. b. s. History and applications of hydrogels. *J Journal of biomedical sciences* **2015**, *4*.

(10) Cascone, S.; Lamberti, G. J. I. J. o. P. Hydrogel-based commercial products for biomedical applications: A review. *J International Journal of Pharmaceutics* **2020**, *573*, 118803.

(11) Singh, R.; Mahto, V. J. P. S. Synthesis, characterization and evaluation of polyacrylamide graft starch/clay nanocomposite hydrogel system for enhanced oil recovery. *J Petroleum Science* **2017**, *14*, 765-779.

(12) Yi, Q.; Tan, J.; Liu, W.; Lu, H.; Xing, M.; Zhang, J. J. C. E. J. Peroxymonosulfate activation by three-dimensional cobalt hydroxide/graphene oxide hydrogel for wastewater treatment through an automated process. *J Chemical Engineering Journal* **2020**, *400*, 125965.

(13) Zhang, L.; Wang, E. J. N. T. Metal nanoclusters: new fluorescent probes for sensors and bioimaging. *J Nano Today* **2014**, *9*, 132-157.

(14) Chen, G.; Tang, W.; Wang, X.; Zhao, X.; Chen, C.; Zhu, Z. J. P. Applications of hydrogels with special physical properties in biomedicine. *J Polymers* **2019**, *11*, 1420.

(15) Wang, Y.; Chang, C.; Zhang, L. J. M. M.; Engineering. Effects of freezing/thawing cycles and cellulose nanowhiskers on structure and properties of biocompatible starch/PVA sponges. *J Macromolecular Materials Engineering* **2010**, *295*, 137-145.

(16) Elhady, M. A.; Elnahas, H.; Meligi, G.; Ammar, A. J. J. o. P. S.; Technology. Study of different methods to induce crosslinking of polyacrylamide for agriculture process. *J Journal of Particle ScienceTechnology* **2019**, *5*, 1-11.

(17) Rusu, D.; Ciolacu, D.; Simionescu, B. C. J. C. C.; TECHNOLOGY. CELLULOSE-BASED HYDROGELS IN TISSUE ENGINEERING APPLICATIONS. *J CELLULOSE CHEMISTRY TECHNOLOGY* **2019**, *53*, 907-923.

(18) Kang, G. D.; Cheon, S. H.; Khang, G.; Song, S.-C. J. E. j. o. p.; biopharmaceutics. Thermosensitive poly (organophosphazene) hydrogels for a controlled drug delivery. *J European journal of pharmaceutics biopharmaceutics* **2006**, *63*, 340-346.

(19) Nho, Y. C.; Lim, Y. M.; Lee, Y. M. J. R. P.; Chemistry. Preparation, properties and biological application of pH-sensitive poly (ethylene oxide)(PEO) hydrogels grafted with acrylic acid (AAc) using gamma-ray irradiation. *J Radiation Physics Chemistry* **2004**, *71*, 239-242.

(20) Liu, H.; Wang, C.; Gao, Q.; Liu, X.; Tong, Z. J. A. b. Magnetic hydrogels with supracolloidal structures prepared by suspension polymerization stabilized by Fe2O3 nanoparticles. *J Acta biomaterialia* **2010**, *6*, 275-281.

(21) Censi, R.; Vermonden, T.; van Steenbergen, M. J.; Deschout, H.; Braeckmans, K.; De Smedt, S. C.; van Nostrum, C. F.; Di Martino, P.; Hennink, W. J. J. o. c. r. Photopolymerized thermosensitive hydrogels for tailorable diffusion-controlled protein delivery. *J Journal of controlled release* **2009**, *140*, 230-236.

(22) Dena, A. S. A.; Ali, A. M.; El-Sherbiny, I. M. Surface-Imprinted Polymers (SIPs): Advanced Materials for Bio-Recognition. *J Natural Sciences Publishing Cor*.

(23) Kiatkamjornwong, S.; Phunchareon, P. J. J. o. a. p. s. Influence of reaction parameters on water absorption of neutralized poly (acrylic acid-co-acrylamide) synthesized by inverse suspension polymerization. *J Journal of applied polymer science* **1999**, *72*, 1349-1366.

(24) Ahmed, E. M. J. J. o. a. r. Hydrogel: Preparation, characterization, and applications: A review *J Journal of advanced research* **2015**, *6*, 105-121.

(25) Flowerlet, M.; Arya, S.; Mini, A.; Nayir, S.; Joseph, J.; Vineetha, V. J. I. J. o. U. P.; Sciences, B. Hydrogel-a drug delivery device. *J International Journal of Universal PharmacyBio Sciences* **2014**, *3*, 2-4.

(26) Aswathy, S.; Narendrakumar, U.; Manjubala, I. J. H. Commercial hydrogels for biomedical applications. **2020**, *6*, e03719.

(27) Kardos, A.; Gilányi, T.; Varga, I. J. J. o. c.; science, i. How small can poly (N-isopropylacrylamide) nanogels be prepared by controlling the size with surfactant? *J Journal of colloid interface science* **2019**, *557*, 793-806.

(28) Cabane, E.; Zhang, X.; Langowska, K.; Palivan, C. G.; Meier, W. J. B. Stimuli-responsive polymers and their applications in nanomedicine. *J Biointerphases* **2012**, *7*, 9.

(29) Huang, H.; Qi, X.; Chen, Y.; Wu, Z. J. S. P. J. Thermo-sensitive hydrogels for delivering biotherapeutic molecules: A review. *J Saudi Pharmaceutical Journal* **2019**, *27*, 990-999.

(30) Jeong, B.; Kim, S. W.; Bae, Y. H. J. A. d. d. r. Thermosensitive sol–gel reversible hydrogels. *J Advanced drug delivery reviews* **2012**, *64*, 154-162.

(31) Wu, C. J. M. A comparison between thecoil-to-globule'transition of linear chains and the “volume phase transition” of spherical microgels. *J Macromolecules* **1998**, *39*, 4609-4619.

(32) Lanzalaco, S.; Armelin, E. J. G. Poly (n-isopropylacrylamide) and copolymers: A review on recent progresses in biomedical applications. *J Gels* **2017**, *3*, 36.

(33) He, H. Multifunctional medical devices based on pH-sensitive hydrogels for controlled drug delivery. The Ohio State University, 2006.

(34) Peppas, N.; Bures, P.; Leobandung, W.; Ichikawa, H. J. E. j. o. p.; biopharmaceutics. Hydrogels in pharmaceutical formulations. *J European journal of pharmaceutics biopharmaceutics* **2000**, *50*, 27-46.

(35) Qiu, Y.; Park, K. J. A. d. d. r. Environment-sensitive hydrogels for drug delivery. *J Advanced drug delivery reviews* **2001**, *53*, 321-339.

(36) Lu, H.; Zhang, N.; Ma, M. J. W. I. R. N.; Nanobiotechnology. Electroconductive hydrogels for biomedical applications. *J Wiley Interdisciplinary Reviews: NanomedicineNanobiotechnology* **2019**, *11*, e1568.

(37) Dehvari, K.; Chen, H.-L.; Garvey, C.; Hong, P.-D. Thermo-Responsive Gold Nanoparticles Platform for Amplification of Cellular Internalization and Photothermal Therapy.

(38) Pich, A.; Richtering, W.: Microgels by precipitation polymerization: synthesis, characterization, and functionalization. In *J Chemical Design of Responsive Microgels*; Springer, 2010; pp 1-37.

(39) Loxley, A.; Vincent, B. J. C.; science, p. Equilibrium and kinetic aspects of the pH-dependent swelling of poly (2-vinylpyridine-co-styrene) microgels. *J Colloid polymer science* **1997**, *275*, 1108-1114.

(40) Kaneda, I.; Vincent, B. J. J. o. c.; science, i. Swelling behavior of PMMA-g-PEO microgel particles by organic solvents. *J Journal of colloid interface science* **2004**, *274*, 49-54.

(41) Gotoh, T.; Nakatani, Y.; Sakohara, S. J. J. o. A. P. S. Novel synthesis of thermosensitive porous hydrogels. *J Journal of Applied Polymer Science* **1998**, *69*, 895-906.

(42) Das, M.; Zhang, H.; Kumacheva, E. J. A. R. M. R. Microgels: Old materials with new applications. *J Annu. Rev. Mater. Res* **2006**, *36*, 117-142.

(43) Rendevski, S. J.; Andonovski, A. N. J. P. B. Reaggregation of sodium alginate microgel structures after shear-induced deaggregation at filtering. *J Polymer Bulletin* **2005**, *54*, 93-100.

(44) Mateus, D.; Alves, S.; Da Fonseca, M. J. B.; bioengineering. Diffusion in cell-free and cell immobilising κ-carrageenan gel beads with and without chemical reaction. *J Biotechnology bioengineering* **1999**, *63*, 625-631.

(45) Dirksen, M.; Dargel, C.; Meier, L.; Brändel, T.; Hellweg, T. J. C.; Science, P. Smart microgels as drug delivery vehicles for the natural drug aescin: uptake, release and interactions. *J Colloid*

Polymer Science **2020**, 1-14.

(46) Wiehemeier, L.; Brändel, T.; Hannappel, Y.; Kottke, T.; Hellweg, T. J. S. m. Synthesis of smart dual-responsive microgels: correlation between applied surfactants and obtained particle morphology. *J Soft matter* **2019**, *15*, 5673-5684.

(47) Jiang, Y.; Colazo, M. G.; Serpe, M. J. In *Tilte*2016; AMER CHEMICAL SOC 1155 16TH ST, NW, WASHINGTON, DC 20036 USA.

(48) Roy, K.; Athiyanathil, S. J. M. P. S. Polymer thermo-responsive gate membranes. *J MOJ Poly Sci* **2017**, *1*, 54-56.

(49) Senff, H.; Richtering, W. J. C.; Science, P. Influence of cross-link density on rheological properties of temperature-sensitive microgel suspensions. *J ColloidPolymer Science* **2000**, *278*, 830-840.

(50) Varga, I.; Gilányi, T.; Mészáros, R.; Filipcsei, G.; Zrinyi, M. J. T. J. o. P. C. B. Effect of cross-link density on the internal structure of poly (N-isopropylacrylamide) microgels. *J The Journal of Physical Chemistry B* **2001**, *105*, 9071-9076.

(51) Najafi, M.; Hebels, E.; Hennink, W. E.; Vermonden, T. J. T.-R. P. C., Properties,; Applications. Poly (N-isopropylacrylamide): Physicochemical Properties and Biomedical Applications. *J Temperature-Responsive Polymers: Chemistry, Properties, Applications* **2018**, 3.

(52) Gilányi, T.; Varga, I.; Mészáros, R.; Filipcsei, G.; Zrínyi, M. J. L. Interaction of monodisperse poly (N-isopropylacrylamide) microgel particles with sodium dodecyl sulfate in aqueous solution. *J Langmuir* **2001**, *17*, 4764-4769.

(53) Costa, M. C.; Silva, S. M.; Antunes, F. E. J. J. o. M. L. Adjusting the low critical solution temperature of poly (N-isopropyl acrylamide) solutions by salts, ionic surfactants and solvents: A rheological study. *J Journal of Molecular Liquids* **2015**, *210*, 113-118.

(54) Plamper, F. A.; Richtering, W. J. A. o. c. r. Functional microgels and microgel systems. *J Accounts of chemical research* **2017**, *50*, 131-140.

(55) Zhang, G.; Wang, D.; Gu, Z.-Z.; Möhwald, H. J. L. Fabrication of superhydrophobic surfaces from binary colloidal assembly. *J Langmuir* **2005**, *21*, 9143-9148.

(56) Bhattacharya, S.; Eckert, F.; Boyko, V.; Pich, A. J. S. Temperature-, pH-, and magnetic-field-sensitive hybrid microgels. *J Small* **2007**, *3*, 650-657.

(57) Pich, A.; Hain, J.; Lu, Y.; Boyko, V.; Prots, Y.; Adler, H.-J. J. M. Hybrid microgels with ZnS inclusions. *J Macromolecules* **2005**, *38*, 6610-6619.

(58) Naseem, K.; Begum, R.; Farooqi, Z. H. J. P. C. Platinum nanoparticles fabricated multiresponsive microgel composites: synthesis, characterization, and applications. *J Polymer Composites* **2018**, *39*, 2167-2180.

(59) Zhu, L.; Li, P.; Gao, D.; Liu, J.; Liu, Y.; Sun, C.; Xu, M.; Chen, X.; Sheng, Z.; Wang, R. J. C. C. pH-sensitive loaded retinal/indocyanine green micelles as an "all-in-one" theranostic agent for multi-modal imaging in vivo guided cellular

senescence-photothermal synergistic therapy. *J Chemical Communications* **2019**, *55*, 6209-6212.

(60) Wang, H.; Xie, J.; Almkhelfe, H.; Zane, V.; Ebini, R.; Sorensen, C. M.; Amama, P. B. J. J. o. M. C. A. Microgel-assisted assembly of hierarchical porous reduced graphene oxide for high-performance lithium-ion battery anodes. *J Journal of Materials Chemistry A* **2017**, *5*, 23228-23237.

(61) Pich, A.; Richtering, W. Polymer nanogels and microgels. **2012**.

(62) Xie, J.; Zheng, Y.; Ying, J. Y. J. J. o. t. A. C. S. Protein-directed synthesis of highly fluorescent gold nanoclusters. *J Journal of the American Chemical Society* **2009**, *131*, 888-889.

(63) Xie, J.; Zheng, Y.; Ying, J. Y. J. J. o. t. A. C. S. Protein-directed synthesis of highly fluorescent gold nanoclusters"J Journal of the American Chemical Society". *J Journal of the American Chemical Society* **2009**, *131*, 888-889.

(64) Dixon, J. M.; Egusa, S. J. J. o. t. A. C. S. Conformational change-induced fluorescence of bovine serum albumin–gold complexes. *J Journal of the American Chemical Society* **2018**, *140*, 2265-2271.

(65) Fehér, B.; Lyngsø, J.; Bartók, B.; Mihály, J.; Varga, Z.; Mészáros, R.; Pedersen, J. S.; Bóta, A.; Varga, I. J. J. o. M. L. Effect of pH on the conformation of bovine serume albumin-gold bioconjugates. *J Journal of Molecular Liquids* **2020**, 113065.

(66) Kinsella, J.; Whitehead, D.: Proteins in whey: chemical, physical, and functional properties. In *Advances in food and nutrition research*; Elsevier, 1989; Vol. 33; pp 343-438.

(67) Einstein, A.: *Investigations on the Theory of the Brownian Movement*; Courier Corporation, 1956.

(68) Technical Committee ISO/TC 24, P. c. i. s. S. S., Particle characterization: *Particle size analysis: dynamic light scattering (DLS)*; ISO, 2017.

(69) Meng, Z. Self-assembly and chemo-ligation strategies for polymeric multi-responsive microgels. Georgia Institute of Technology, 2009.

(70) Quigley, R.; Barnard, P. A.; Hussey, C. L.; Seddon, K. R. Electrochemical and spectroscopic characterization of niobium {Nb6Cl12} z+ chloride clusters in the aluminum chloride-1-methyl-3-ethylimidazolium chloride molten salt. *Inorganic Chemistry* **1992**, *31*, 1255-1261.

(71) Utane, R.; Ansari, M.; Deo, S.; Inam, F. UV-Visible Determination of Synthetic Compound 1-Phenyl Naphthalene and Extracted Plant Lignans Derivatives.

(72) Clark, B.; Frost, T.; Russell, M.: *UV Spectroscopy: Techniques, instrumentation and data handling*; Springer Science & Business Media, 1993; Vol. 4.

(73) Greenwood, R.; Kendall, K. J. J. o. t. E. C. S. Electroacoustic studies of moderately concentrated colloidal suspensions. *J Journal of the European Ceramic Society* **1999**, *19*, 479-488.

(74) Hanaor, D.; Michelazzi, M.; Leonelli, C.; Sorrell, C. C. J. J. o. t. E. C. S. The effects of carboxylic acids on the aqueous dispersion and electrophoretic deposition of ZrO2. *J Journal of the European Ceramic Society* **2012**, *32*, 235-244.

(75) Drioli, E.; Giorno, L.: *Encyclopedia of membranes*; Springer, 2018.

(76) Dolghih, E. Theoretical Studies of Dye-labeled DNA Systems with Applications to Fluorescence Resonance Energy Transfer. University of Florida, 2009.

(77) Pereira, A. S.; Tavares, P.; Limão-Vieira, P.: *Radiation in Bioanalysis: Spectroscopic Techniques and Theoretical Methods*; Springer Nature, 2019; Vol. 8.

(78) Naresh, K. J. J. C. P. S. Applications of fluorescence spectroscopy. *J J. Chem. Pharm. Sci* **2014**, *974*, 2115.

(79) Wu, Y.; Li, H.; Rao, Z.; Li, H.; Wu, Y.; Zhao, J.; Rong, J. J. J. o. M. C. B. Controlled protein adsorption and delivery of thermosensitive poly (N-isopropylacrylamide) nanogels. *J Journal of Materials Chemistry B* **2017**, *5*, 7974-7984.

(80) Shang, J.; Gao, R.; Su, F.; Wang, H.; Zhu, D. J. A. i. P. T. Colloidal Probes of PNIPAM-Grafted SiO2 in Studying the Microrheology of Thermally Sensitive Microgel Suspensions. *J Advances in Polymer Technology* **2020**, *2020*.